12-1-1978

Bench-Scale Study of Sulfur and Nitrogen Oxides Absoption by Nahcolite and Trona

Frederick R. Stern

BENCH-SCALE STUDY OF SULFUR AND NITROGEN OXIDES ADSORPTION BY NAHCOLITE AND TRONA.

by
Frederick R. Stern
Bachelor of Arts, Dickinson State College 1975

A Thesis
Submitted to the Graduate Faculty
of the
University of North Dakota
in partial fulfillment of the requirements
for the degree of
Master of Science

Grand Forks, North Dakota
December
1978

This thesis submitted by Frederick R. Stern in partial fulfillment of the requirements for the Degree of Master of Science from the University of North Dakota is hereby approved by the Faculty Advisory Committee under whom the work has been done.

Wayne R Burke
(Chairman)

William J. Lawrence

Everett A. Boutwell

Dean of the Graduate School

Permission

Title Bench-Scale Study of Sulfur and Nitrogen Oxides Adsorption by Nahcolite and Trona

Department Chemical Engineering

Degree Master of Science

In presenting this thesis in partial fulfillment of the requirements for a graduate degree from the University of North Dakota, I agree that the Library of this University shall make it freely available for inspection. I further agree that permission for extensive copying for scholarly purposes may be granted by the professor who supervised my thesis work or, in his absence, by the Chairman of the Department or the Dean of the Graduate School. It is understood that any copying or publication or other use of this thesis or part thereof for financial gain shall not be allowed without my written permission. It is also understood that due recognition shall be given to me and to the University of North Dakota in any scholarly use which may be made of any material in my thesis.

Signature Frederick R. Stern

Date 12-1-78

ACKNOWLEDGEMENTS

The author wishes to express appreciation to the Association of Western Universities, Salt Lake City, Utah, the Grand Forks Energy Technology Center, United States Department of Energy, Grand Forks, North Dakota, and the University of North Dakota, Grand Forks, North Dakota for the fellowship under which this work was done.

Special gratitude is expressed to Professor Wayne R. Kube and Dr. Everett A. Sondreal, Grand Forks Energy Technology Center, for their invaluable guidance throughout this project. Thanks is also extended to W. Fred Lawrence, Chairman of the Management Department, for reviewing this thesis.

The author wishes to thank Messrs. Harvey M. Ness, Stanley J. Selle, Gerald M. Goblirsch, and Dr. Franklin I. Honea of the Grand Forks Energy Technology Center Staff for their guidance and assistance.

Special thanks to Donald L. West, John D. Hilley, and Ronald R. Brown for their assistance in construction and maintenance of experimental equipment.

Appreciation is also expressed to Douglas Slowiak for his work on illustrations and to Rosemary T. Honek for typing the thesis.

TABLE OF CONTENTS

TABLE OF CONTENTS--Continued

LIST OF TABLES

LIST OF ILLUSTRATIONS

LIST OF ILLUSTRATIONS--Continued

ABSTRACT

The extent and rates of sulfur and nitrogen oxides 'dry' adsorption by nahcolite and trona were measured. Experiments were conducted by passing simulated flue gas through a fixed bed of test material. Variables considered in the study were particle size, reaction temperature, concentration of sulfur dioxide, and concentration of water vapor in the flue gas.

High reaction rates were noted for the adsorption of sulfur dioxide by nahcolite at reaction temperatures of 400-650° F and for particle diameters of 0.19 mm or less. Based on the adsorption of sulfur dioxide, certain tests resulted in nahcolite utilizations of over 95 pct. Trona also proved to be capable of adsorbing sulfur dioxide. However, reaction rates and utilizations were considerably lower. Neither nahcolite or trona proved to be an effective adsorbent of nitrogen oxide. Water vapor concentrations of 5 to 15 volume percent had no significant effect on reaction rates or utilizations. For the nahcolite-sulfur dioxide reaction both chemical reaction and gas diffusion through the ash layer mechanisms contributed major resistances in controlling the overall reaction rate.

The high reaction rates and utilizations determined for the nahcolite-sulfur dioxide reaction indicate that nahcolite has great potential as a sorbent for 'dry' flue gas desulfurization.

INTRODUCTION

The reduction of sulfur dioxide (SO_2) emissions to the atmosphere is considered an environmental problem in the United States as well as other industrialized nations. In 1975, over 35 million tons of SO_2 were discharged from industrial sources in the U.S., with electric power generation utilizing fossil fuels contributing nearly 60 pct of the total emissions (1).

The following environmental regulations apply to fossil-fuel combustion emissions: the U.S. Environmental Protection Agency (EPA) is presently enforcing a New Source Performance Standard (NSPS) and National Ambient Air Quality Standard (NAAQS) of 1.2 lb. SO_2 emitted per million Btu input and 80 micrograms SO_2 per cubic meter (annual mean concentration for a 24-hr. period) respectively (2,3). Other state and local governmental agencies, such as Clark County, Nevada and the State of Wyoming, have adopted even more stringent performance standards for new electrical generating units. In addition, the EPA at this time (August 1978) is considering NSPS revisions requiring removal of 85 pct or more of the total sulfur input (4).

These regulations have resulted in research and development (R&D) programs directed at removing SO_2 from stack gases so as to meet the standards. From these efforts, several methods of SO_2 removal have resulted. A very adequate listing and description of these methods are given by Slack and Holliden (5).

Methods presently available for SO_2 removal are generally termed either 'wet' or 'dry' and 'regenerative' or 'throw away'. Wet methods utilize a slurry or solution in a gas-liquid contacting system which may be a spray or packed tower. 'Dry' techniques use dry adsorbent particles in a gas-solid contacting system, such as a moving bed or a baghouse. Salable sulfur compounds are produced from the reacted adsorbent in a regenerative system and the reclaimed adsorbent is returned to the sulfur removal system. The spent adsorbent is disposed of without regeneration in 'throw away' methods.

In recent years nahcolite, a natural occurring form of sodium bicarbonate, and trona, a natural occurring form of sodium carbonate and sodium bicarbonate, have received considerable attention as possible adsorbents for SO_2 removal in 'dry' throwaway systems. Previous investigations have shown nahcolite and trona to be capable of removing 75-90 pct of the SO_2 in a baghouse application (6,7). It is thought that these materials could be utilized in other 'dry' removal systems as well and would, therefore, be of great value in water-scarce areas such as are often found in the Western United States.

Although raw nahcolite and trona are presently unavailable commercially, there are large resources of these materials. The U.S. Bureau of Mines estimates 30 billion tons of nahcolite in the Piceance Creek Basin of Colorado, and trona reserves of 85 billion tons in the Green River formation of Colorado and Wyoming (8). Possible development of oil shale deposits and future changes in economic conditions may cause nahcolite and trona to be available at relatively low prices. The availability of these materials would allow their use for SO_2 removal systems.

RESEARCH PLAN

The objectives of this investigation were to measure and evaluate the sulfur dioxide and nitrogen oxide adsorption properties of the dry sorbents, nahcolite and trona, including the kinetics of sulfur dioxide adsorption by nahcolite. The sulfur dioxide adsorption capability of trona was to be evaluated at more limited conditions only for comparison with nahcolite.

In order to obtain a definable system with a consistent sorbent surface area, pretreatment of the sorbents was required by thermal activation. The parameters investigated were reaction temperature, particle size, concentration of sulfur dioxide, and concentration of water vapor in the simulated flue gas. The concentration level of nitric oxide was held constant for all tests.

STATUS AND COMPARISON OF FLUE GAS DESULFURIZATION SYSTEMS

At the present time all flue gas desulfurization (FGD) units in utility service are 'wet' processes. The most widely and best developed of these processes are lime/limestone systems (see Table 1). It is expected that lime/limestone systems will continue to dominate utility FGD units for several years because of the more favorable economics of this process. Some other promising 'wet' FGD processes are listed in Table 2.

TABLE 1

FLUE GAS DESULFURIZATION UNITS IN U.S. (9)

Status	No. of units	MW	Percentage of units (by MW) lime/limestone
Operational.....	30	6,476	92
Under construction.....	31	13,309	86
Planned:			
Contract awarded.....	20	9,981	98
Letter of intent.....	2	365	52
Requesting/evaluating bids.....	4	2,327	14
Considering FGD systems.....	37	16,726	26
TOTAL.....	124	49,184	-

TABLE 2

FLUE GAS DESULFURIZATION PROCESSES HAVING POTENTIAL FOR UTILITY APPLICATION

Process	Sorbent Used	Type
Lime/limestone	Lime or limestone	Wet-Throw away
Double Alkali	Sodium hydroxide/lime	Wet-Throw away
Wellman-Lord	Sodium sulfite	Wet-Regenerative
Citrate	Sodium citrate, citric acid, and sodium thiosulfate	Wet-Regenerative
Shell	Copper	Dry-Regenerative
Foster Wheeler-Forschung	Activated char	Dry-Regenerative

Presently there are no actual 'dry' FGD processes available that have been proven on a full scale basis. However, a semi-'dry' process, developed by Rockwell International Corp., is to be used on Montana Dakota Utilities et al. Coyote Station at Beulah, ND (10). Rockwell's Spray Dryer process utilizes a system in which the water is evaporated from an aqueous solution of sodium carbonate by hot flue gases leaving dry solid particles. The partial listing of available FGD processes in Table 2 includes two other potential 'dry' methods.

Although 'dry' methods of flue gas desulfurization are not presently in use, certain economical and operational advantages exist over the 'wet' methods. A study by Dulin et al. (6) in 1973 investigated the economics of a nahcolite injection-baghouse FGD system for the cases of a

Southwestern and a Midwestern electrical generating plant. The investigation included a comparison of capital and annual costs for the nahcolite system versus a 'wet' limestone FGD system. The basis for this economic analysis are given in Table 3 and the results of this comparison are summarized in Table 4.

TABLE 3

BASIS FOR ECONOMIC ANALYSIS COMPARING
SO_2 REMOVAL SYSTEMS FOR TWO POWER PLANTS

	Southwestern Power Plant	Midwestern Power Plant
SO_2 removal efficiency, %.....	70	75
Delivered nahcolite cost, $/ton.....	23.80	19.00
Delivered limestone cost, $/ton.....	10.00	3.00

TABLE 4

SUMMARY OF ESTIMATED COSTS FOR SO_2 REMOVAL
PROCESSES FOR TWO POWER PLANTS IN 1973 DOLLARS (6)

	Southwestern Power Plant (one 800 MW unit)		Midwestern Power Plant (two 840 MW units)	
Item	Nahcolite Injection	Wet Limestone Scrubbing	Nahcolite Injection	Wet Limestone Scrubbing
Capital Cost:				
$ MM.....	15.8	25.8	45.2	66.7
$/kw.....	19.8	32.2	26.9	39.7
Annual Cost:				
$ MM.....	8.42	7.8	35.6	27.1
$/ton coal burned...	3.36	3.11	7.66	3.66
mills/kwh.....	1.77	1.64	3.72	2.83
¢/10^6 Btu.....	18.6	17.2	36.5	27.0
$/ton S removed.....	676	625	292	215

The nahcolite system represents a substantial savings in capital costs for each case. It should be noted that the figures in Table 4 are in terms of 1973 dollars and that plant costs have now increased approximately 51 pct (11). However, assuming that inflation has had an equal effect on all aspects of plant cost, a capital cost savings of 38.6 pct for the Southwestern plant and 32.2 pct for the Midwestern plant could be realized by the nahcolite system. The annual costs of the nahcolite system were higher than those of the limestone system for both cases, but only slightly so for the plant in the southwest. The lower annual cost of the limestone systems can be directly attributed to the lower transportation costs of raw limestone.

The capital cost advantage for the nahcolite system is offset by the higher annual costs for a plant in the midwest. However, in the case of the Southwestern plant the annual costs are similar and the nahcolite system is able to economically compete with the limestone system.

The economic feasibility for a nahcolite system depends on location of the plant. For areas where nahcolite sources are near to the plant site a nahcolite FGD system would be economically viable. Whereas the limestone system would have an economic advantage for plants realizing low transportation costs for the limestone ore.

Systems utilizing dry adsorbents other than nahcolite may have greatly different economic characteristics and need to be evaluated on an individual basis.

'Dry' methods of FGD have a number of distinct operational advantages over 'wet' methods. A major advantage of a 'dry' system is that no water is required. This eliminates problems associated with the handling and disposal of wet sludges. The absence of water requirements would also be of particular benefit for plants located in water scarce areas.

Another advantage of 'dry' FGD is that the SO_2 adsorption occurs at relatively high temperatures. Wet SO_2 removal systems operate at the adiabatic saturation temperature of the absorbent solution and require flue gas reheat or bypass to obtain satisfactory flue-gas buoyancy. Other problems inherent in most 'wet' systems or 'scrubbers', but avoided in 'dry' systems, are: 1) scrubber scaling, 2) demister plugging, and 3) equipment damage due to corrosion and abrasion.

An operational disadvantage of most 'dry' methods does exist; a 'dry' system must generally be operated at a higher pressure drop than that of a 'wet' system in order to obtain similiar SO_2 removal efficiencies. It should be noted that this single factor alone may dictate whether or not a 'dry' method is acceptable for situations where high SO_2 removal efficiencies are required.

Another problem associated with the use of dry sorbents containing sodium is disposal of the spent sorbent. Leaching of sodium from these water soluble compounds to groundwater sources must be controlled. One means of dealing with this problem is to chemically insolubilize the spent sorbent prior to disposal to land fill. A second solution is to line the land-fill site with plastic or clay.

THEORETICAL ASPECTS OF ADSORPTION

Description of Adsorption

Adsorption is generally defined as the condensation of a gas or vapor on the surface of a porous solid. The phenomena of adsorption is explained by considering the surface molecules of a solid particle. The atoms of a surface molecule have no like atoms above the surface plane with which to form a chemical bond. The unbalanced surface molecule thus exhibits an inward attraction which can be satisfied by adsorbing a gaseous or liquid molecule on to the solid surface. Two types of adsorption are known to exist--physical adsorption and chemisorption (12).

In physical adsorption, Van der Waal's forces attract the adsorbed species to the solid surface. No chemical reaction takes place and since the Van der Waal forces are relatively weak the process is often reversible. Generally low activation energies are required and the adsorption occurs only at temperatures less than the boiling point of the adsorbed species (adsorbate).

In the case of chemisorption, an actual chemical reaction occurs between the adsorbent and the adsorbate resulting in forces much greater than the Van der Waal forces of physical adsorption. The chemisorption process is generally considered irreversible and usually requires high activation energies. Chemisorption differs from physical adsorption also in that the rate of chemisorption is in most cases significantly

increased at higher temperatures. Since chemisorption is mainly responsible for gas-solid reactions, the remainder of this section will deal with factors affecting and describing chemisorption.

Surface Area, Activation, and Structural Changes

A factor that affects the rate of adsorption is the number of active sites available for reaction. Langmuir related the number of sites to surface area and proposed that the rate of adsorption was directly proportional to the fractional portion of the surface area not covered by adsorbate (13). If Θ is the fraction of the surface area covered by adsorbate, the rate of adsorption per unit surface area, r_a, is given as

$$r_a = k_a P_A(1-\Theta) \qquad [1]$$

where,

k_a= rate constant

P_A= partial pressure of the adsorbate

The rate of desorption is directly proportional to the surface area covered by adsorbate expressed by Equation [2].

$$r_d = k_d\Theta \qquad [2]$$

The rates of adsorption and desorption are equal at equilibrium and the fraction of the surface area covered at equilibrium conditions is given by Equation [3].

$$\Theta = \frac{k_a P_A}{k_d + k_a P_A} \qquad [3]$$

The equilibrium expression of Equation [3] is often referred to as Langmuir's adsorption isotherm (13).

Brunauer, Emmett, and Teller (BET) further developed the principles of Langmuir to obtain a scheme for measuring the specific surface area of a solid (13). Use of the BET isotherm allows the surface area to be determined by measuring the volume of nitrogen adsorbed on a known weight of material at various pressures. Surface area measurements made in this study were based on the BET isotherm.

The specific surface area of a solid depends to a great extent on the pore development of the material. Materials such as activated carbon have a high degree of pore development and thus a large surface area per unit mass. According to Equation [1], a solid with a large surface area per unit mass should have high rates of adsorption. This statement, however, does not hold true in all instances. In some cases many of the pore openings of a material are smaller than the adsorbate molecule and the surface area within the pore is unavailable for reaction.

One method of promoting pore development in solids is thermal activation. In thermal activation, the heated material releases volatile matter or thermal decomposition products leaving void area within the solid particle. The thermal activation of nahcolite and trona is accomplished by the decomposition of sodium bicarbonate to sodium carbonate as shown in Equation [4].

$$2\ NaHCO_3 \xrightarrow[\Delta]{} Na_2CO_3 + H_2O + CO_2,\ \Delta H = +31\ \text{kcal/g mole} \qquad [4]$$

The surface area of activated materials may be several orders of magnitude greater than the surface area of the starting material. In some

cases the activation process proceeds so rapidly and violently that large cracks as well as pores are formed resulting in somewhat higher surface areas.

When heat treating solids, other structural changes, which have a diminishing effect on surface area, can occur. One of the most common unwanted structural changes is known as the sintering phenomena. The sintering effect usually begins to take place at a temperature of 0.4 to 0.5 times the absolute melting point temperature of the solid and proceeds more rapidly at higher temperatures (13). In sintering, the necks of the grains within a particle contact and as this contact area grows the pores between the grains are diminished in size and eventually the pores are closed entirely. A schematic presentation of the sintering effect is given in Figure 1 (13).

Chemisorption Models

Selecting a chemisorption model which closely corresponds to the actual case is the first step in developing a reaction rate expression. Proper model selection will lead to a rate expression capable of fitting experimental data and predicting the actual kinetics. In the study of gas-solid reactions involving particles of unchanging size, two reaction models are generally discussed (12). The continuous-reaction model is applied to cases in which the adsorbate enters the particle and reacts throughout the total particle volume. Figure 2 is a schematic presentation of particle conversion in the continuous-reaction model (12).

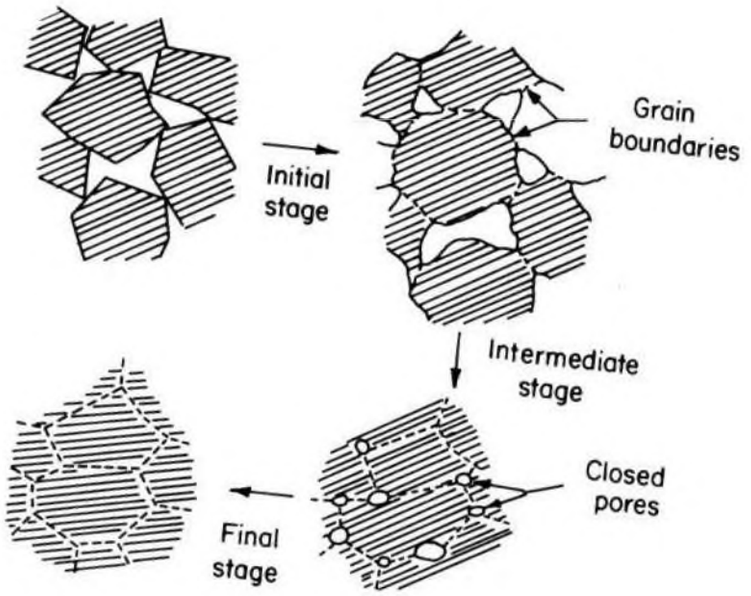

Figure 1. - The progressive stages of sintering.

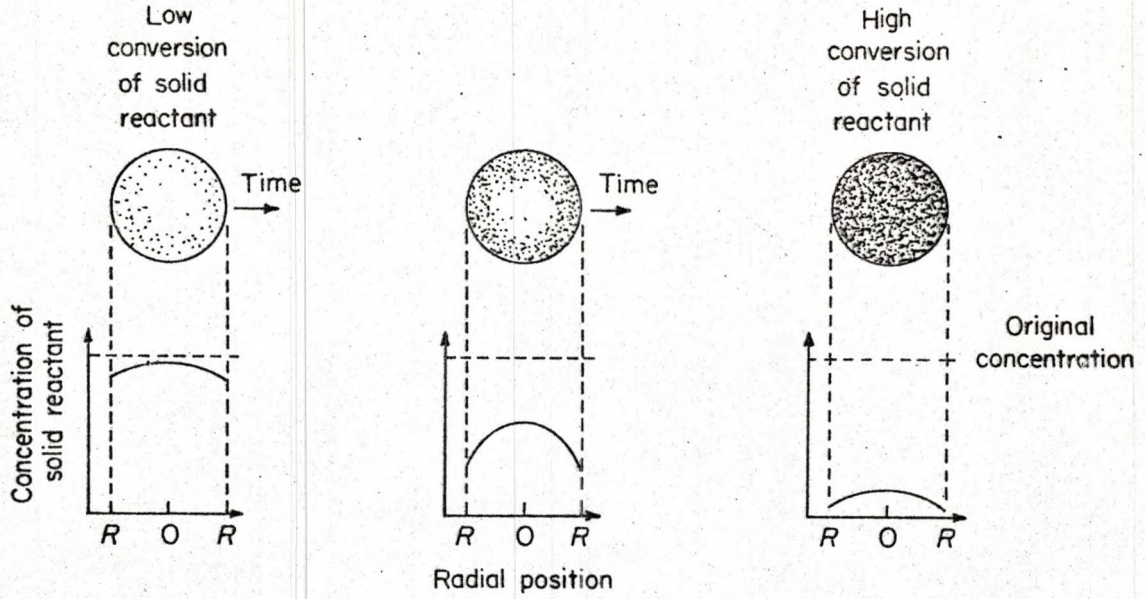

Figure 2. - Reaction progression in a continuous reaction model.

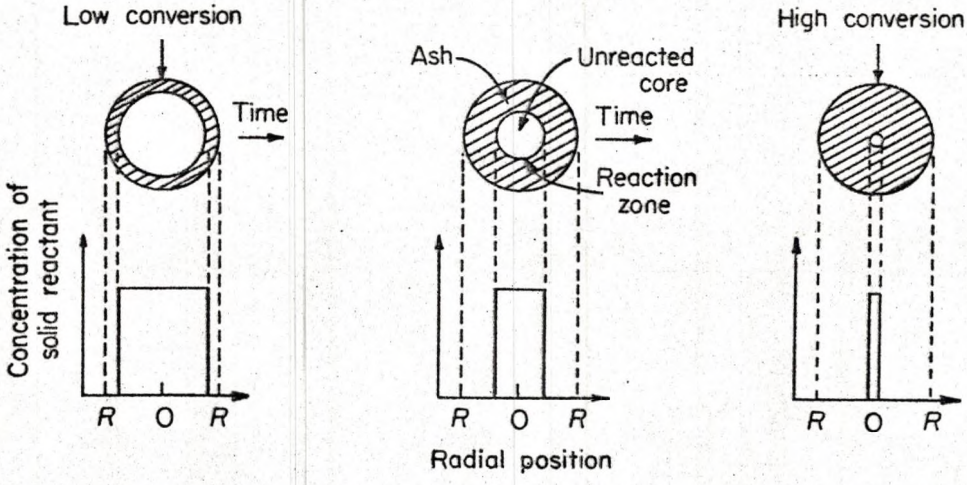

Figure 3. - Ash layer development according to the unreacted-core model.

In the unreacted-core model, often referred to as the shrinking-core model, the reaction occurs first at the particle surface. The reaction then proceeds inward leaving behind a zone of completely reacted material termed 'ash'. This 'ash' layer, which for the compounds of this study is Na_2SO_4, thickens as the reaction proceeds and in some cases offers considerable resistance to adsorbate diffusion into the particle. The progress of particle conversion in an unreacted-core model is presented in Figure 3 (12).

Although the continuous-reaction model fits certain cases well, the unreacted-core model best represents actuality in most instances (12). The unreacted-core model seems more representative of the actual physical case in the present work, and will therefore be used in describing the kinetics of SO_2 adsorption by nahcolite.

Rate Controlling Steps

In order to obtain a reaction rate expression having physical significance, it is often necessary to determine which step or combination of steps offer the major reaction resistance. It should be noted that a determined rate controlling step is only valid for specified experimental conditions. Varying the particle size, gas velocity, temperature, or other parameters may cause a different step to become rate controlling.

Levenspiel (12) indicates five possible rate controlling steps exist for the reaction of a gas with a particle of unchanging size. These steps are as follows:

STEP 1. - Gas phase diffusion of gaseous reactant A.

STEP 2. - Diffusion of gaseous reactant A through the ash layer of the particle.

STEP 3. - Chemical reaction.

STEP 4. - Diffusion of gaseous products back through the ash layer.

STEP 5. - Gas phase diffusion of gaseous products.

Since the reaction of activated nahcolite and trona with SO_2, given by

$$Na_2CO_3 + SO_2 + 1/2\ O_2 \rightarrow Na_2SO_4 + CO_2,\ \Delta H = -85\ kcal/g\ mole \quad [5]$$

is considered to be irreversible up to approximately 1,500° F, Steps 4 and 5 can be eliminated from the list of possible rate controlling steps for this study (12). The following expressions, given by Levenspiel, mathematically describe progression of the reaction according to the remaining possible rate controlling steps.

Case 1. - Controlling Step - Gas Film Diffusion

$$\frac{t}{\tau} = 1 - \left(\frac{r_c}{R}\right)^3 = X_B \quad [6]$$

Case 2. - Controlling Step - Diffusion through Ash

$$\frac{t}{\tau} = 1 - 3\left(\frac{r_c}{R}\right)^2 + 2\left(\frac{r_c}{R}\right)^3 = 1 - 3(1-X_B)^{2/3} + 2(1-X_B) \quad [7]$$

Case 3. - Controlling Step - Chemical Reaction

$$\frac{t}{\tau} = 1 - \frac{r_c}{R} = 1 - (1 - X_B)^{1/3} \quad [8]$$

where,

t = time, sec.

r_c= radius of unreacted core, cm

R = radius of particle, cm

X_B= conversion of sorbent at any time, t

τ = time for complete reaction, sec.

The rate controlling step can then be identified by comparing experimental kinetic data with the curves predicted by Equations [6], [7] and [8]. A plot of $(1-X_B)$ versus t/τ, given in Figure 4 (12), serves this purpose.

Determination of the rate controlling step may not be straightforward. The curves predicted by Equations [7] and [8] are very similiar and experimental scatter could cause difficulty in determining whether Step 2 or Step 3 is rate controlling. Also, it is possible that one step may be rate controlling for a portion of the reaction and that another step may become controlling as the reaction progresses. One means of distinguishing whether chemical reaction or ash diffusion is rate controlling is to do kinetic runs at several temperatures. Since the effect of temperature is generally much more significant for chemical reaction than for diffusion, a large change in reaction rate with respect to temperature would indicate chemical reaction to be rate controlling.

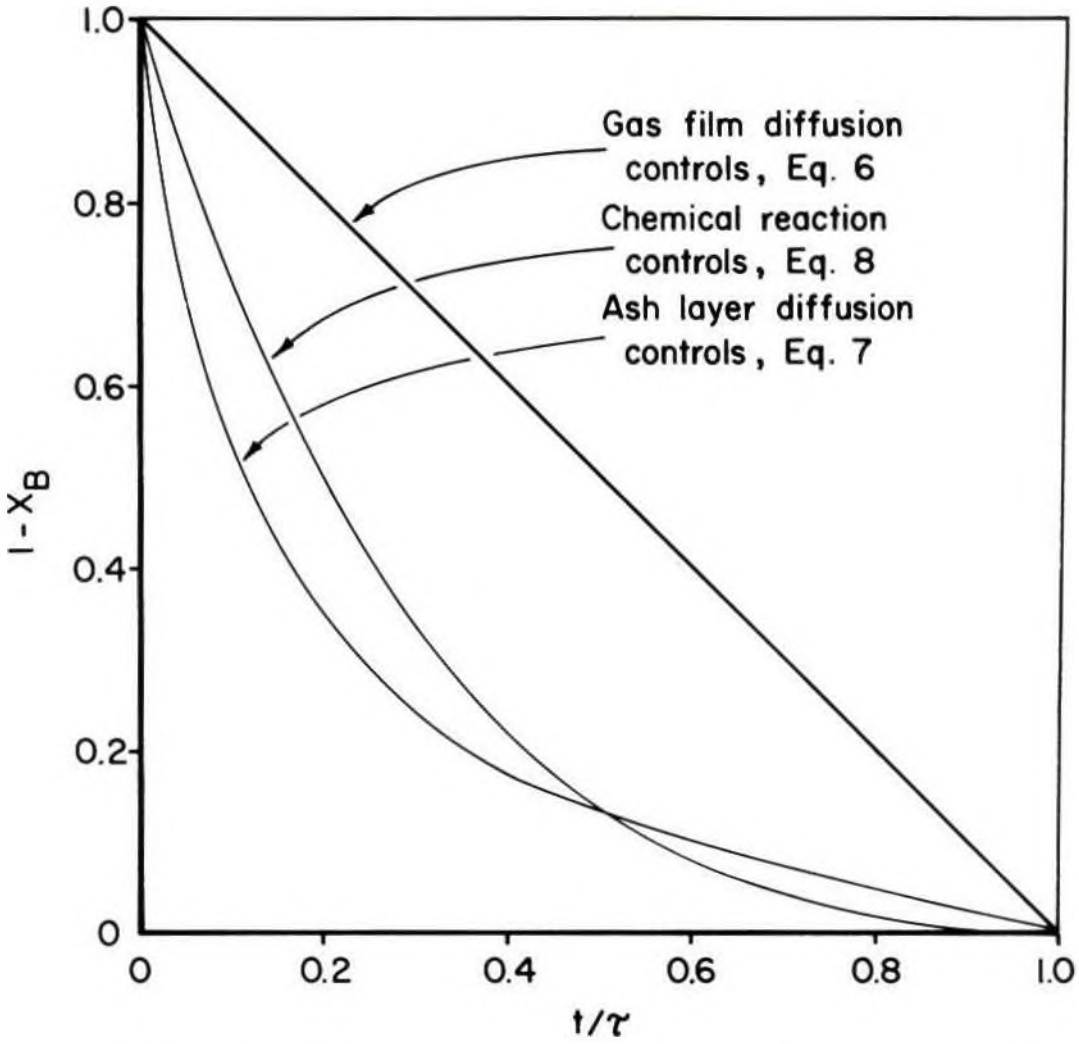

Figure 4. - Reaction progress predicted by various rate controlling steps.

Rate Expression Determination

After a rate controlling step or steps have been determined, application of Equations [9], [10], and [11] should allow the rate of reaction to be described and predicted (12). In order to obtain an overall expression that represents the actual case over a wide portion of the reaction, it may be necessary to combine or modify Equation [9], [10], and [11].

Case 1. - Controlling Step - Gas Film Diffusion

$$\frac{dN_A}{4\pi R^2\, dt} = k_g C_{Ag}^m \qquad [9]$$

Case 2. - Controlling Step - Diffusion Through Ash

$$\frac{dN_A}{dt}\left(\frac{1}{r_c} - \frac{1}{R}\right) = 4\,\pi\, D\, C_{Ag}^m \qquad [10]$$

Case 3. - Controlling Step - Chemical Reaction

$$\frac{dN_A}{4\pi r_c^2\, dt} = k_s C_{Ag}^m \qquad [11]$$

where,

N_A = gram moles of A in sorbent at any time, t

k_g = rate constant (gas diffusion controlling), cm/sec

k_s = rate constant (chemical reaction controlling), cm/sec

D = diffusivity of gas through ash layer, cm^2/sec

C_{Ag} = concentration of A in gas phase, g $mole/cm^3$

m = order of reaction with respect to A

For a chemical reaction of the form $aA + bB \rightarrow cC + dD$, X_B, the conversion of the sorbent is given as

$$X_B = \frac{b(N_A - N_{AO})}{aN_{BO}} \qquad [12]$$

The radius of the unreacted core, r_c, is generally not known, but for particles related to the unreacted-core model it is expressed by

$$r_c = R(1 - X_B)^{1/3} \qquad [13]$$

Regardless of which case is shown to be the controlling step for a particular set of conditions, it will be necessary to evaluate m, the order of reaction. This can be accomplished by determining the reaction rate, $\frac{dN_A}{dt}$, at several concentration levels of A in the gas. The reaction rate is obtained by plotting (gram moles of A)/(gram of sorbent) versus reaction time. Measuring the tangent to the data curves then directly provides $\frac{dN_A}{dt}$ as (gram moles of A)/(gram sorbent - sec). Having obtained the reaction rate for several levels of C_{Ag}, a plot of log $\frac{dN_A}{dt}$ versus log C_{Ag} is made. The resultant slope is then equal to the order of reaction.

EQUIPMENT

A differential-type fixed bed reactor was chosen as the gas-solid contacting device in preference to a fluidized-bed reactor to insure no particle attrition during experimental tests (14). Four identical fixed bed reactors were constructed of 304 stainless steel. Each reactor had an overall length of 12 inches and an inside diameter of 2.0 inches. The reactors were designed such that the bed depth could be varied from 0.125 inch to 1.75 inch. A sintered stainless steel disc served as the sorbent support screen and gas distribution plate. In order to maintain a fixed bed, an identical sintered disc and a tubular spacer were placed directly above the sorbent. Reactor details are presented in Figure 5.

Reactor preheat and adiabatic conditions were accomplished by the use of Samox insulated electrical heating jackets. The four reactors with heating jackets were housed in an insulated container. A photograph of the reactor bank is given in Figure 6. Several of the heating jackets, rated at 1,000 watts each, failed during operation. Failures were attributed to poor heater-reactor contact and to power surges from the on-off temperature controllers. After fastening the heaters to the reactors more securely and limiting the set point differential of the temperature controller to 10° F, no additional heater failures were experienced.

In preparing simulated flue gas, a temperature controlled water bath was used to humidify an inert gas (approximately 85 volume percent

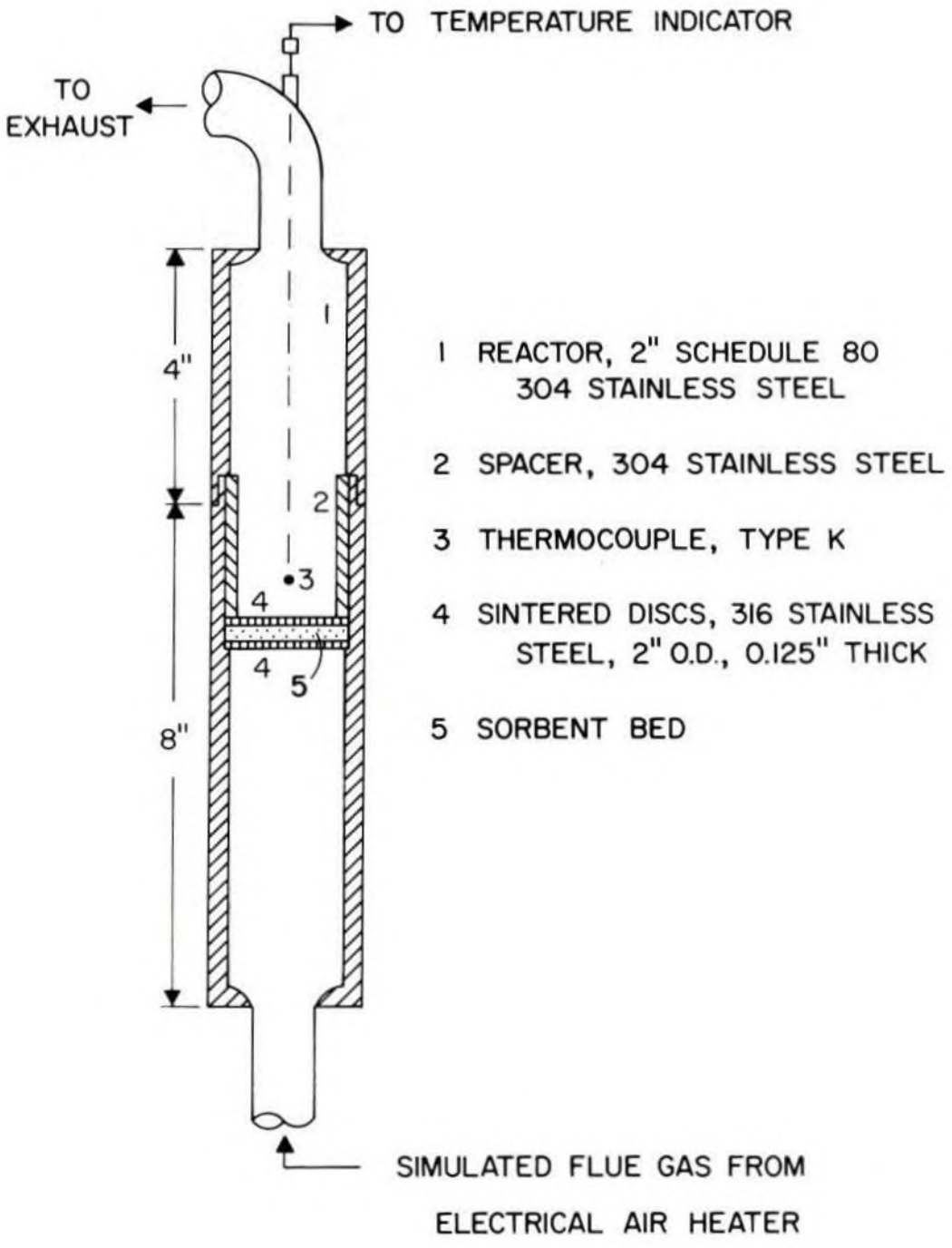

Figure 5.- Fixed-bed reactor.

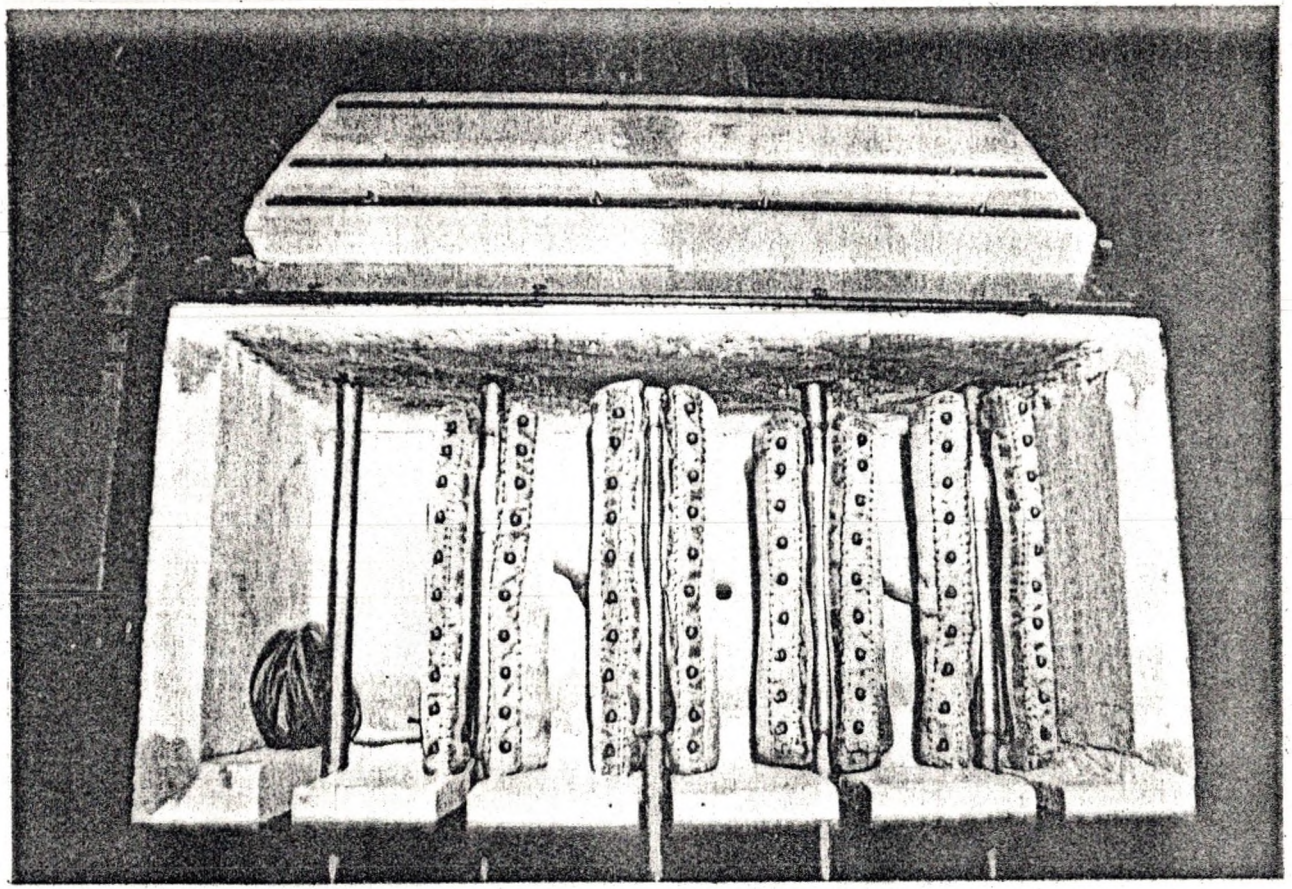

Figure 6. - Reactor Bank.

nitrogen and 15 volume percent carbon dioxide). The flow rates of oxygen, sulfur dioxide, and nitric oxide injected into the main gas stream were controlled by manual adjustments of needle valves. A flange tap orifice meter was used to measure the flue gas flow rate.

An electrical air heater, constructed at the Grand Forks Energy Technology Center (GFETC), was used to heat the simulated flue gas. The heater was designed to deliver flue gas at temperatures up to 1,200° F for a maximum flow rate of 20 standard cubic feet per minute. Thirty Watlow 'Firerod' cartridges, powered by a 3 phase, 208 volt electrical source, provided 15,000 watts of heat input to the heater. Figure 7 presents an illustration of the electrical air heater.

The experimental equipment was housed in the GFETC mobile instrument trailer. The trailer, designed for field testing of power plant type facilities, contains a complete flue gas sampling and analysis system as well as a 'wet' chemical laboratory. Several minor alterations of the trailer's gas analysis system allowed the reactor inlet and outlet gas compositions to be continuously monitored. The electronic gas analyzers used are listed in Table 5 and a view of the instrument panel is given in Figure 8.

TABLE 5

ELECTRONIC INSTRUMENTATION USED FOR FLUE GAS ANALYSIS

Gas analyzed	Manufacturer and model	Type	Accuracy, % of range
Sulfur dioxide	DuPont 400	Ultraviolet	± 2
Nitrogen oxides	Thermo Electron Corp. Series 10	Chemiluminescent	± 0.5
Carbon dioxide	Beckman 864	Infrared	± 1
Oxygen	Beckman 742	Electrochemical	± 1

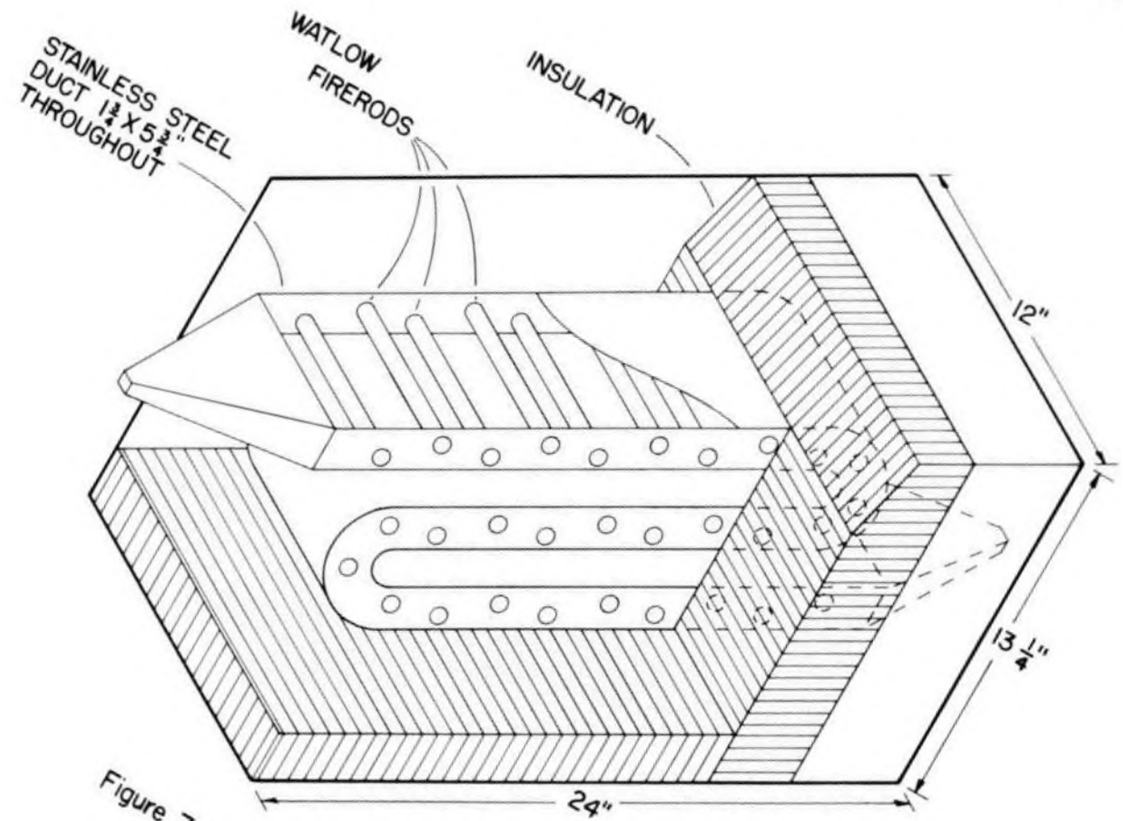

Figure 7.- Electrical Air Heater

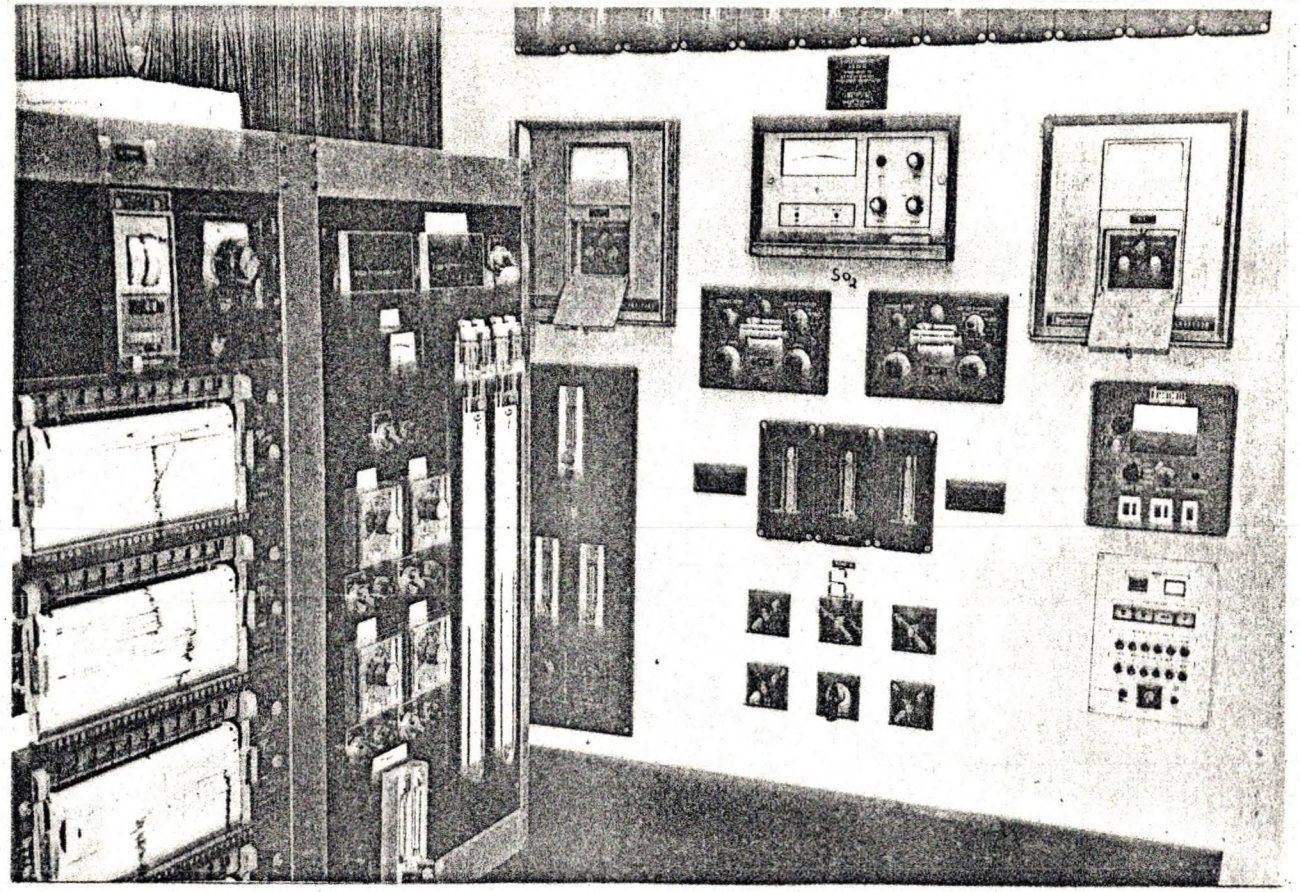

Figure 8.- Instrument Panel.

TEST MATERIALS AND PROCEDURES

Nahcolite was provided by the Utah Power and Light Co., who obtained the material from the Superior Oil Co., Denver, Colorado. The Stauffer Chemical Co. of Wyoming, Green River, Wyoming provided the trona. The nahcolite was mined in the Green River Formation of Colorado and the trona was mined in Wyoming. The nahcolite assayed approximately 70 pct sodium bicarbonate and 7 pct sodium carbonate. The composition of the trona was determined to be approximately 42 pct sodium carbonate and 30 pct sodium bicarbonate. Compositions and physical properties of the starting materials are given in Appendix A.

The nahcolite and trona were crushed to -1/8 inch particles in a hammer mill. The test materials were classified into desired particle size ranges using a Ro-Tap sieve apparatus. To obtain a more definable system, the sized fractions of the nahcolite and trona were pretreated by thermal activation at 600° F for 10 minutes in a forced draft oven. (The activation of the materials are described in the Results and Discussion section.)

A 3.0 gram sample of the sized activated test material was placed in a test reactor resulting in a nominal bed height of 0.125 inches for all tests. After being assembled, the reactor was preheated to a temperature above the dew point of the flue gas to prevent moisture

condensation. Heated inert gas was introduced into the reactor and the temperature of the reactor was increased to the desired reaction temperature. A gas flow rate of approximately 10.5 scfm as determined by the orifice meter was then set by adjustment of the pressure regulator. The selected volume percentage of moisture was obtained by regulating the temperature of the water bath. (Calculations for the gas flow rate calibration and for moisture additions are given in Appendix B.)

The inert gas flow was then diverted to an empty reactor. Sulfur dioxide and nitric oxide were injected into the inert gas stream and flow rates adjusted to give the desired concentration levels as indicated by the gas analyzers. The injection of sulfur dioxide and nitric oxide was halted, and the inert gas flow returned to the test reactor. After the reaction temperature had again been established in the test reactor, the actual experimental test proceeded by injecting sulfur dioxide and nitric oxide at the determined flow rates for a specified test time. The system was then purged of sulfur dioxide and nitric oxide and the reactor was allowed to cool. This procedure was repeated in turn for each of the other test reactors. A complete flow chart of the experimental process is given in Figure 9.

After the test reactor had been disassembled, the sample was recovered, placed in a sealed glass sample vial, and retained for analysis. Descriptions and calculations of the methods used for analysis of the sorbent are given in Appendix C.

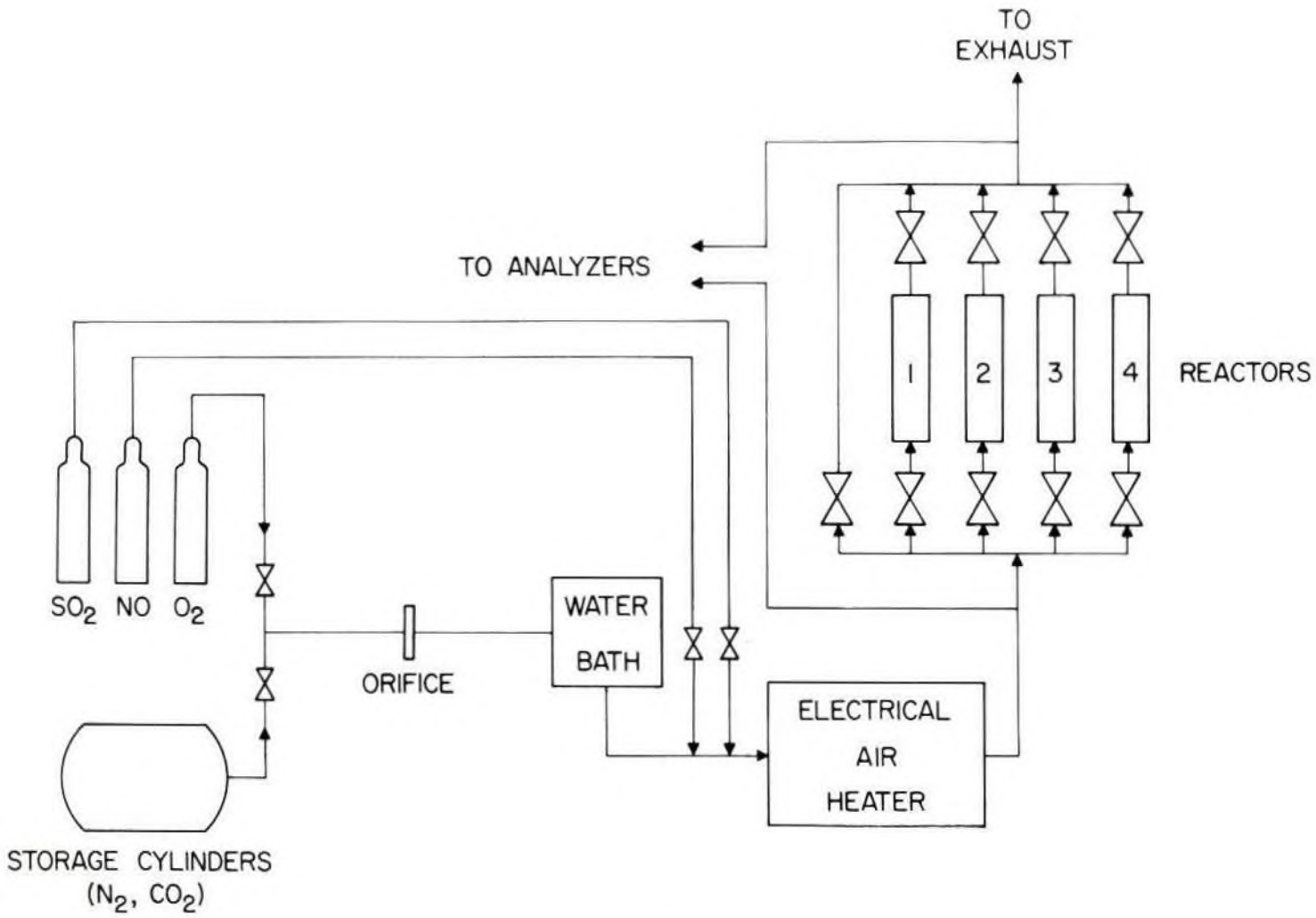

Figure 9. - Flow diagram for study of SO_2 adsorption.

Five replicate runs were conducted to determine reproducibility of the experimental procedure. It was found that 95 pct of the experimental values were within 4 pct of the average values for the five tests (see Appendix B).

Calibration of the electronic gas analyzers was performed before and after each test series, which consisted of six experiments. The analyzers were zeroed by purging with nitrogen and spanned with calibration gases having concentration levels within the experimental test range. Meter outputs gave direct readings of gas concentrations for all analyzers except the Beckman 742 carbon dioxide analyzer. A calibration curve for the Beckman 742 analyzer is given in Appendix D.

The accuracy of the DuPont 400 sulfur dioxide analyzers was periodically checked by comparison with a wet method of sulfur dioxide gas analysis. A modified version of the Shell-Thornton method was used for this comparison (15). Details of and calculations by this method are given in Appendix D.

A set of tests conducted on nahcolite served as a standard reference. The conditions of these tests were as follows:

1. Reaction temperature of 500° F.
2. Mean particle diameter of 0.191 mm.
3. Flue gas concentration levels of:
   a. 1500 ppm SO_2 (wet).
   b. 1000 ppm NO (wet).
   c. 10 vol. pct H_2O.

Other experimental tests conducted are identified by run numbers described by a code system presented in Table 6.

TABLE 6

INTERPRETATION OF RUN NUMBERS

X - Y - Z - T

X - Parameter varied from reference test

1. Reaction temp., °F
2. Particle size, $\overline{Dp}$, mm
3. Water vapor concentration, vol pct.
4. Sulfur dioxide concentration, ppm.

Y - Sorbent tested

A. Nahcolite
B. Trona

Z - Numerical value of parameter variable

T - Reaction time, sec.

SAMPLE: Run 1 - A - 650 - 350 is a test investigating the effect of temperature on nahcolite at 650° F for a reaction time of 350 sec.

CALCULATION OF REACTION RATES AND SORBENT UTILIZATION

The basis for the results discussed are the plots of SO_2 adsorbed per gram activated sorbent versus time and plots of NO adsorbed per gram activated sorbent versus time. A sample set of the calculations used in determining the data points presented in these figures are given in Appendix B. The data was found to closely fit a curve of the mathematical form

$$y = ae^{-(b/t)} \qquad [14]$$

where a and b are constants, y is the milligrams of SO_2 adsorbed per gram activated sorbent, and t is the reaction time in seconds. A least squares linear regression technique was applied to obtain from the data an equation which would allow direct differentiation. Values obtained from the regression analysis are presented in Appendix B.

The rate of SO_2 adsorption was calculated by taking the derivative of Equation [14], giving;

$$\text{rate} = \frac{dy}{dt} = \frac{abe^{-(b/t)}}{t^2} \qquad [15]$$

where $\frac{dy}{dt}$ is the mg SO_2 adsorbed per gram activated sorbent per second. Substitution of the linear regression values given in Table 10, Appendix B, allowed for direct calculation of the adsorption rate at any reaction time, t.

Based on the stoichiometry of Equation [5], the percentage of sorbent utilization was calculated as follows:

$$\% \text{ Utilization} = \frac{\left(\frac{SO_2 \text{ adsorbed}}{\text{g activated sorbent}}\right)\left(\frac{\text{gmol } SO_2}{64\text{g } SO_2}\right)\left(\frac{\text{gmol } Na_2CO_3}{\text{g mol } SO_2}\right)(100)}{\left(\frac{\text{g } Na_2CO_3}{\text{g activated sorbent}}\right)\left(\frac{\text{g mol } Na_2CO_3}{106\text{ g } Na_2CO_3}\right)}$$

RESULTS AND DISCUSSION

General Test Results

A summary of the results for each of the experimental tests is listed in Table 11, Appendix B. Figures 16, 19, 22, 23, 25, and 26 indicate the amount of SO_2 adsorbed with respect to reaction time. Similar plots of NO adsorption are given in Figures 27 and 28. All adsorption numbers given were calculated on an activated sorbent basis.

Evaluation of the test results indicate nahcolite to be more reactive toward SO_2 than trona. The optimum reaction rate of SO_2 with nahcolite was found to occur at a temperature of 650° F. Increased sorbent utilization and higher reaction rates were observed in tests using sorbent material of small particle sizes. Additionally, although only small amounts of NO were adsorbed, nahcolite appeared to be more reactive with NO than trona.

Effects of various variables, identification of rate controlling steps, and application of an overall reaction rate expression are discussed in the following subsections.

Sorbent Activation

A series of tests in which nahcolite was heated for 2 hours at various temperatures indicated maximum pore development to occur between 275° F and 600° F. Heat treatment at temperatures above 600° F actually caused the specific surface area of nahcolite to be greatly diminished

as illustrated in Figure 10. Scanning electron miscroscope (SEM) photos, Figures 11-14, verify this pore development and illustrate the sintering process.

The observed initial sintering temperature of approximately 600° F falls into the predicted sintering temperature range of 350-600° F (based on the melting point temperature of pure sodium carbonate).

Since a high specific surface area was desirable for this study, further activation tests were conducted in the 275-600° F range. The maximum specific surface area of approximately 9.0 m^2/g for -100 mesh nahcolite was obtained at an activation temperature of 600° F (Figure 15). Howitson et al. (16) reported a high rate of pore development at 600° F, but also stated that activation at lower temperatures resulted in an end product of similar surface area. Howitson's report of end products having a similar specific surface area is not supported by this study.

The pore development of trona followed a pattern similar to that of nahcolite, but resulted in a specific surface area approximately 30 pct less (Figure 15). The smaller specific surface area of trona is attributed to the lower concentration of $NaHCO_3$ available for thermal decomposition.

Effect of Temperature on SO_2 Adsorption

It was expected that the nahcolite utilization and reaction rate would increase as the reaction temperature increased. However, as shown in Figure 16, the amount of SO_2 adsorbed in a 10 minute period was virtually the same at reaction temperatures of 400-750° F. In order to obtain a similar utilization of approximately 75 pct, a much longer reaction time would be required at 300° F.

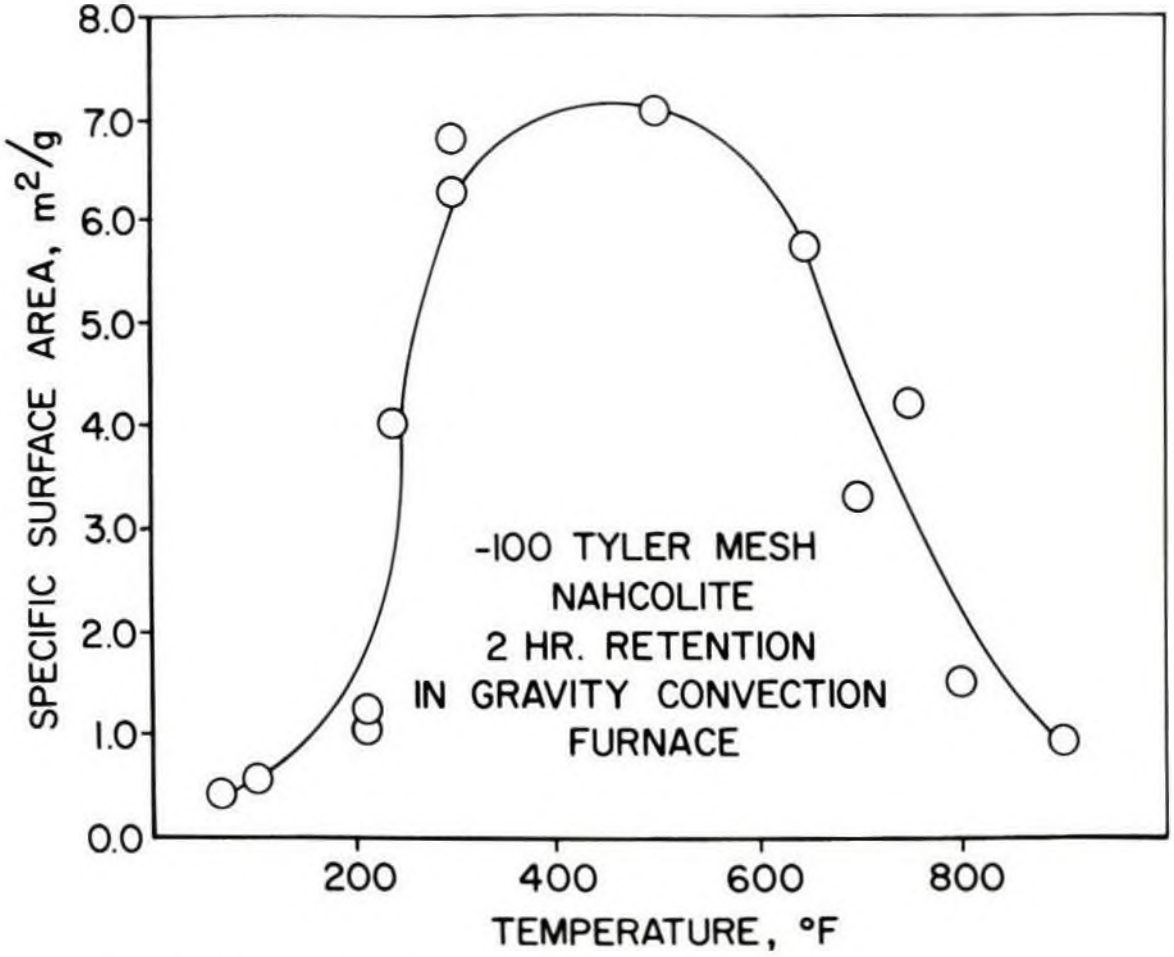

Figure 10. - Effect of extended heating on the surface area of nahcolite.

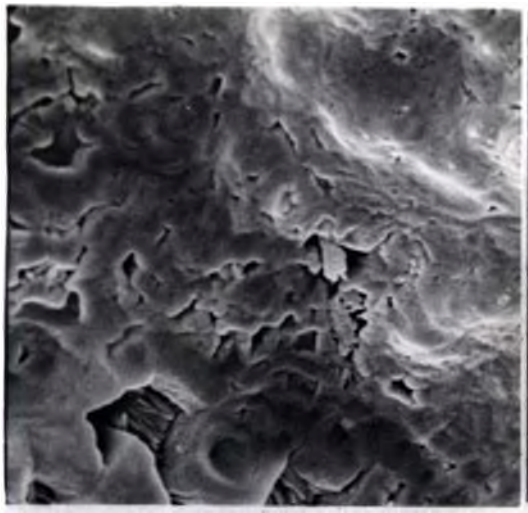

FIGURE 11. – Raw nahcolite – no pore development.

20μm

FIGURE 12. – Nahcolite treated at 600 °F – good pore development. (Two hour treatment.)

20μm

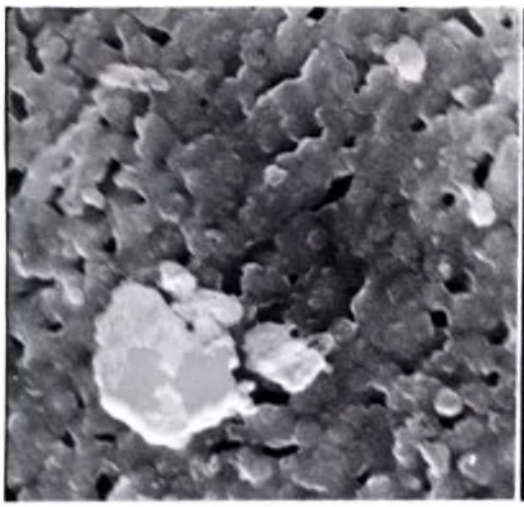

FIGURE 13. – Nahcolite treated at 800 °F – intermediate stages of sintering. (Two hour treatment.)

20μm

FIGURE 14. – Nahcolite treated at 900 °F – final stage of sintering. (Two hour treatment.)

20μm

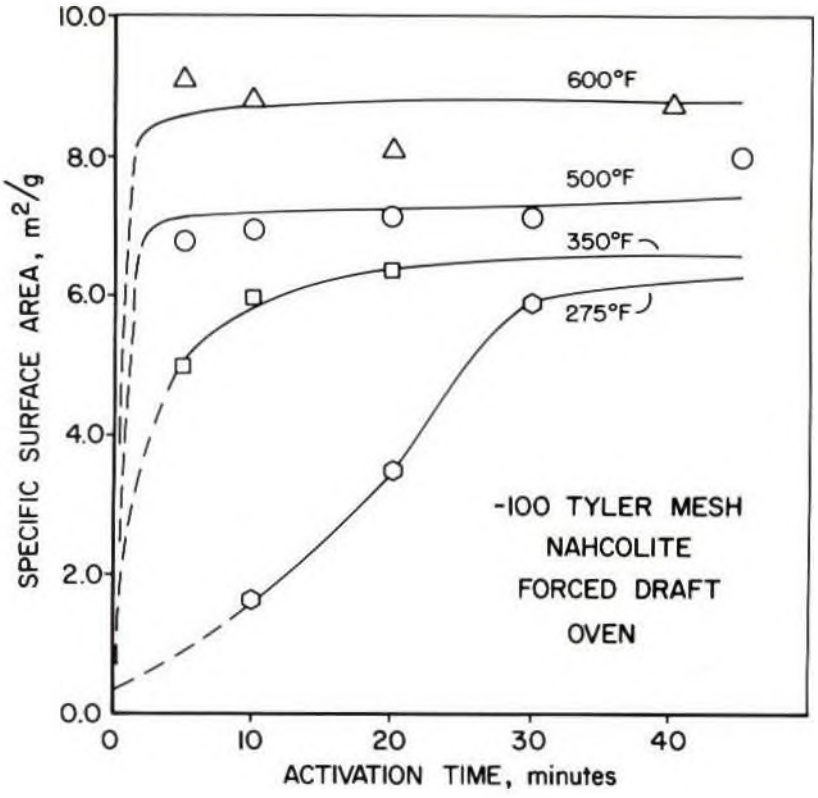

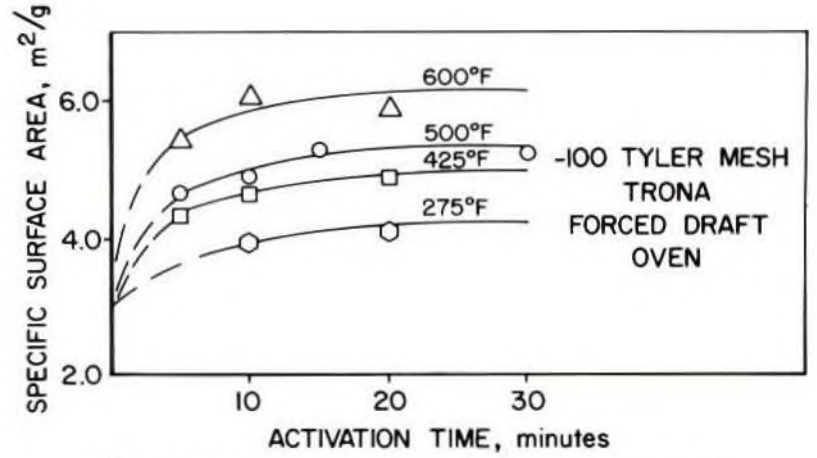

Figure 15.- Results of nahcolite and trona activation tests.

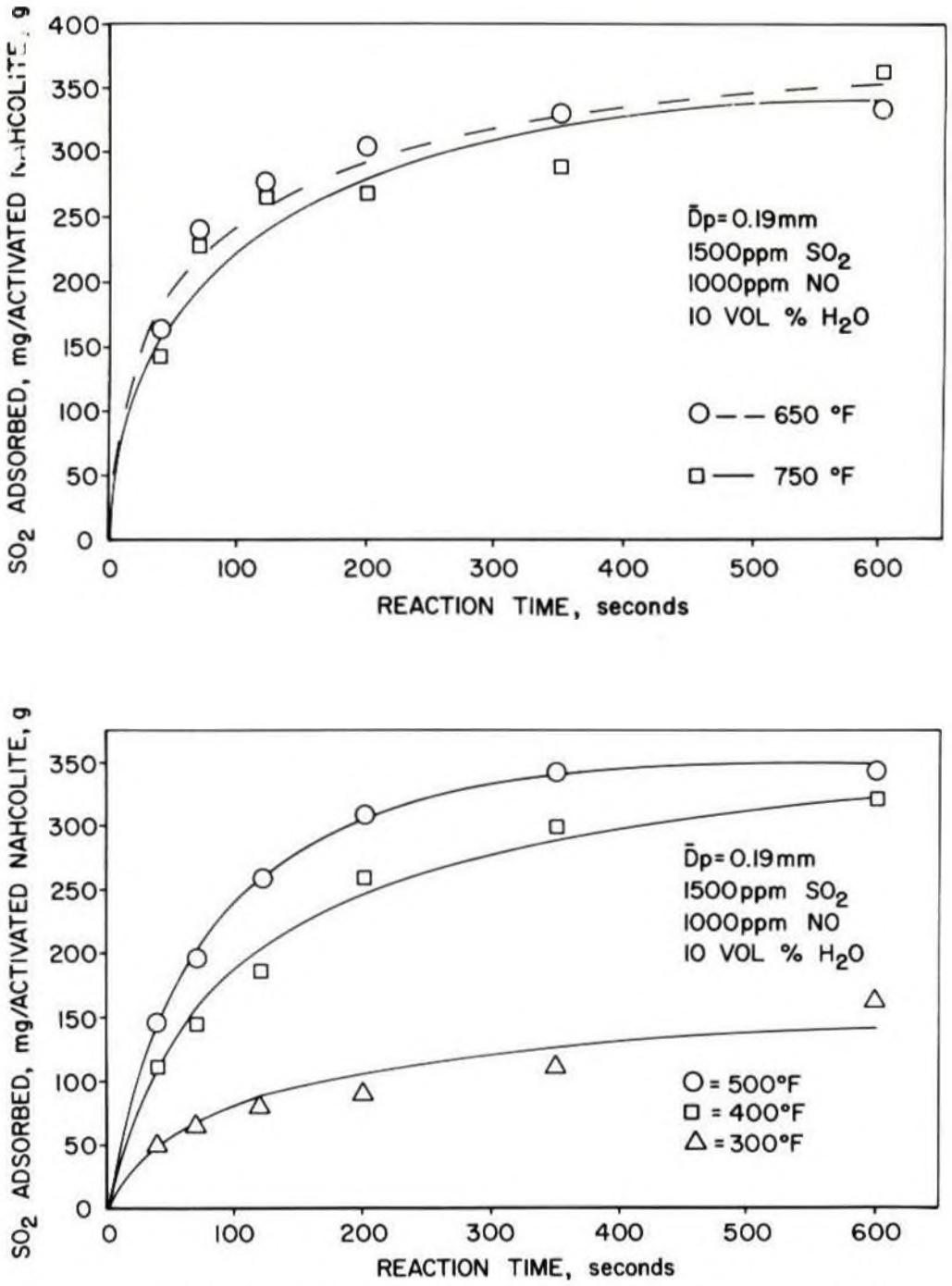

Figure 16. - Temperature effect on adsorbance of SO_2 on nahcolite.

The reaction rate increased rapidly with temperature, but reached a maximum at 650° F (Figure 17). The lower reaction rate at 750° F is attributed to the greatly reduced surface area caused by sorbent sintering at this temperature. Since the reaction rate is much higher at temperatures above 300° F, a more effective SO_2 removal system could be obtained by operating at higher temperatures. The notably higher reaction rates at increased temperatures indicate that chemisorption is the process by which nahcolite adsorbs sulfur dioxide temperatures. Figure 17 also illustrates that nahcolite possesses a relatively high reaction rate at levels of low sorbent conversion and short reaction times.

In order to calculate the activation energy of the nahcolite-SO_2 reaction an Arrhenius plot was made (Figure 18). Since the reaction rate values given at 650° and 750° F may have been affected by sorbent sintering, these two points were excluded in determining the slope of the plot. The activation energy determined in this manner was calculated to be 10,470 cal/g mole. This value compares well with activation energies given for the reaction of SO_2 with similar compounds (17) (Calculations for the Arrhenius equation are given in Appendix B).

Effect of Particle Size

Figure 19 shows the adsorbance of SO_2 versus time for three particle size ranges of nahcolite. The higher reactivity for smaller particles was expected because of the higher surface area to particle weight ratio for small particles.

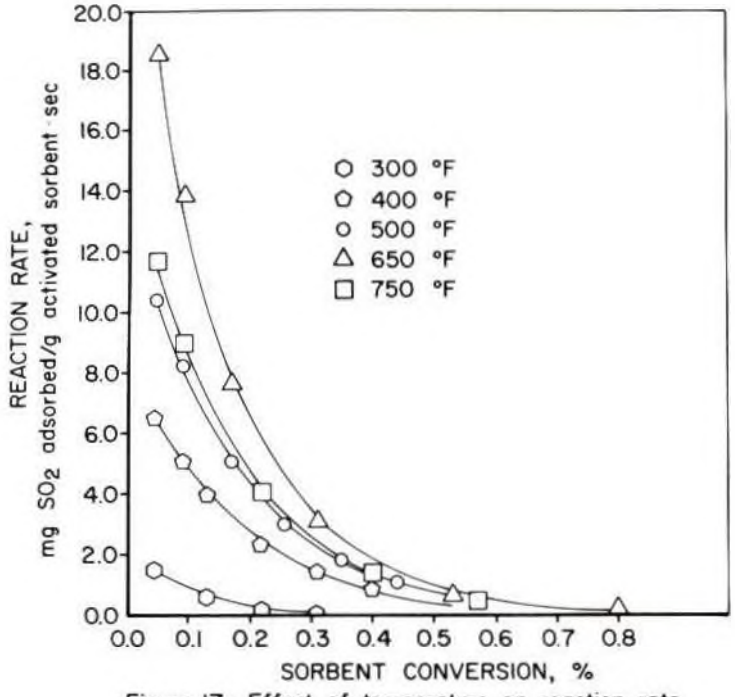

Figure 17. - Effect of temperature on reaction rate.

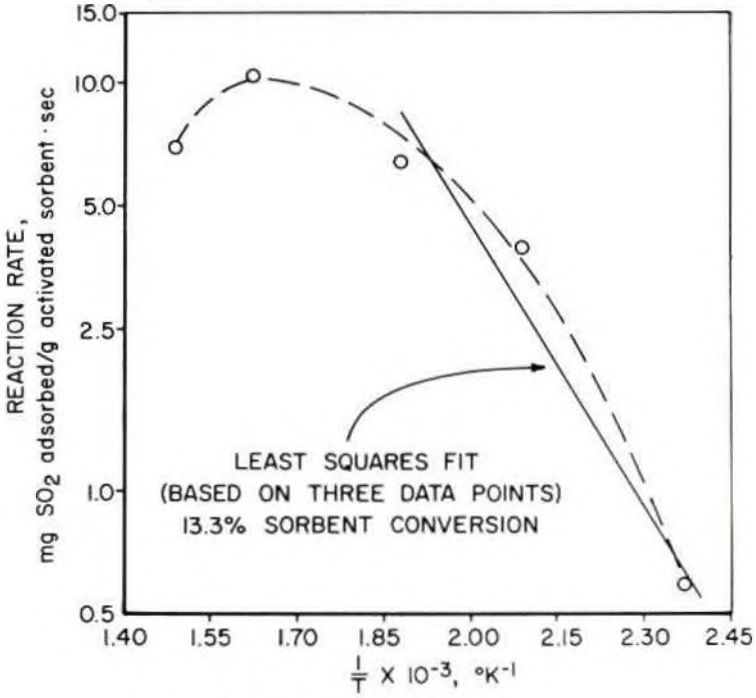

Figure 18. - Arrhenius Plot

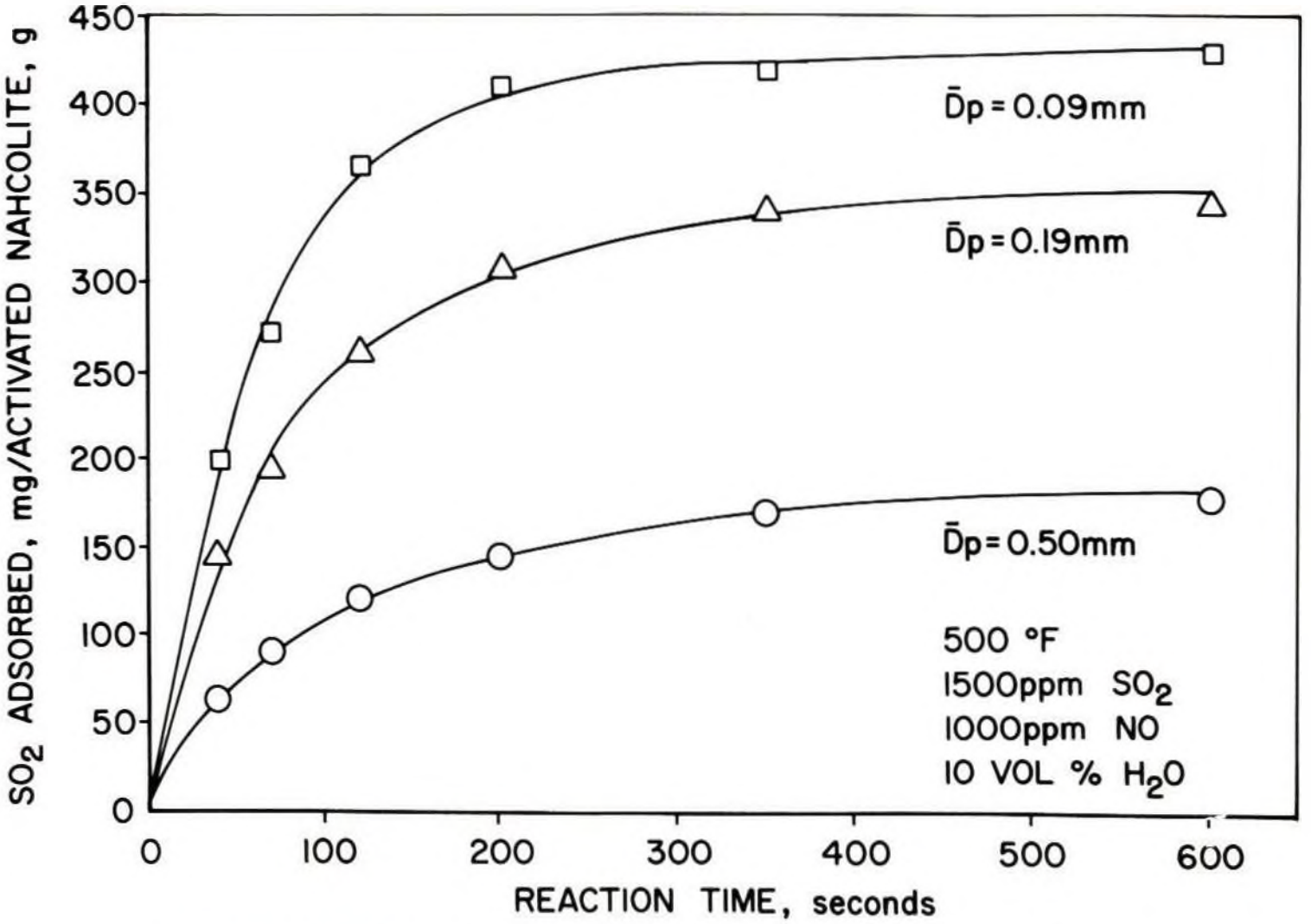

Figure 19.- Particle size effect on SO_2 adsorbance.

An excellent sorbent utilization of approximately 98 pct was observed for the 0.09 mm diameter particles. Conversion of the large particles, however, was considerably less. The lesser extent of conversion for these particles is readily apparent in the SEM photos of cleaved nahcolite particles. Figure 20 is a view of a 0.19 mm diameter particle and Figure 21 is a 0.50 mm particle. The gray area along the surface of each particle is the sodium sulfate 'ash' layer. Both particles had been exposed to SO_2 for 10 minutes and in each case the reacted depth is approximately 0.07 mm. According to Figure 19 the advancement of the 'ash' layer beyond this depth and therefore the rate of additional sorbent conversion will be very slow. The reduced rate of conversion at this 'ash' layer depth is thought to be due to pore blockage by sodium sulfate.

It should be emphasized that the sharp sodium sulfate interfaces shown in Figure 20 and 21 suggest the conversion of nahcolite proceeds as described by the unreacted-core model. The selection of the unreacted core model is further confirmed by the nearly total absence of sulfur in the particle's interior core as determined by X-ray fluorescence (18).

Effect of Flue Gas Moisture

The effect of flue gas moisture on the adsorption of SO_2 is shown in Figure 22. No significant change in reaction rate or nahcolite utilization was observed at 500° F for flue gas moisture levels of 5 to 15 vol pct. It should be noted that testing of the flue gas moisture effect was very limited. Based on the data presented here, it is not possible to predict the effect of flue gas moisture at lower reaction temperatures.

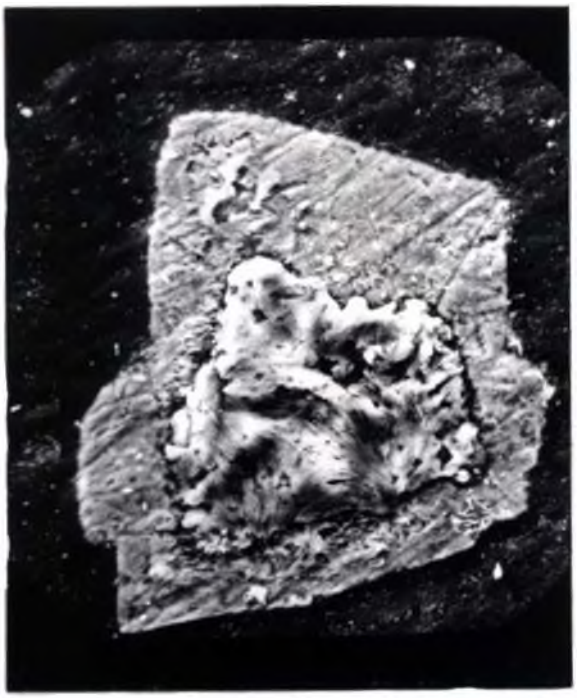

FIGURE 20. – 0.19mm diameter cleaved particle of nahcolite. Reacted for 10 minutes, 500 °F.

100μm

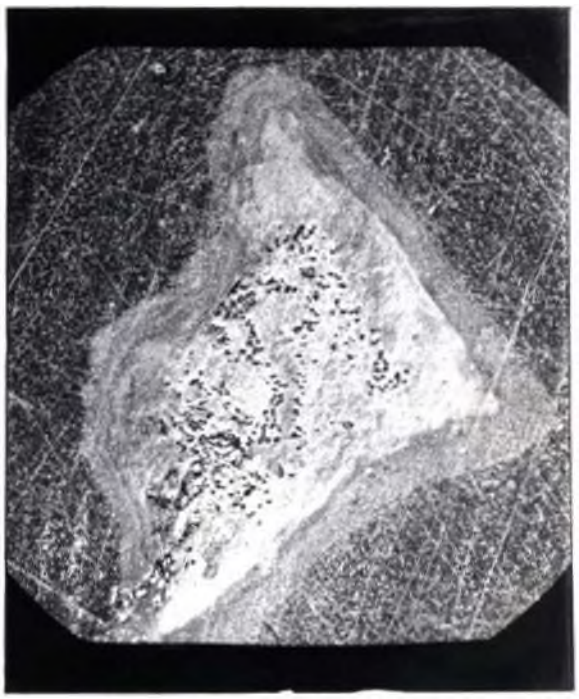

FIGURE 21. – Cleaved nahcolite particle of 0.50mm diameter. Reacted for 10 minutes, 500 °F.

100μm

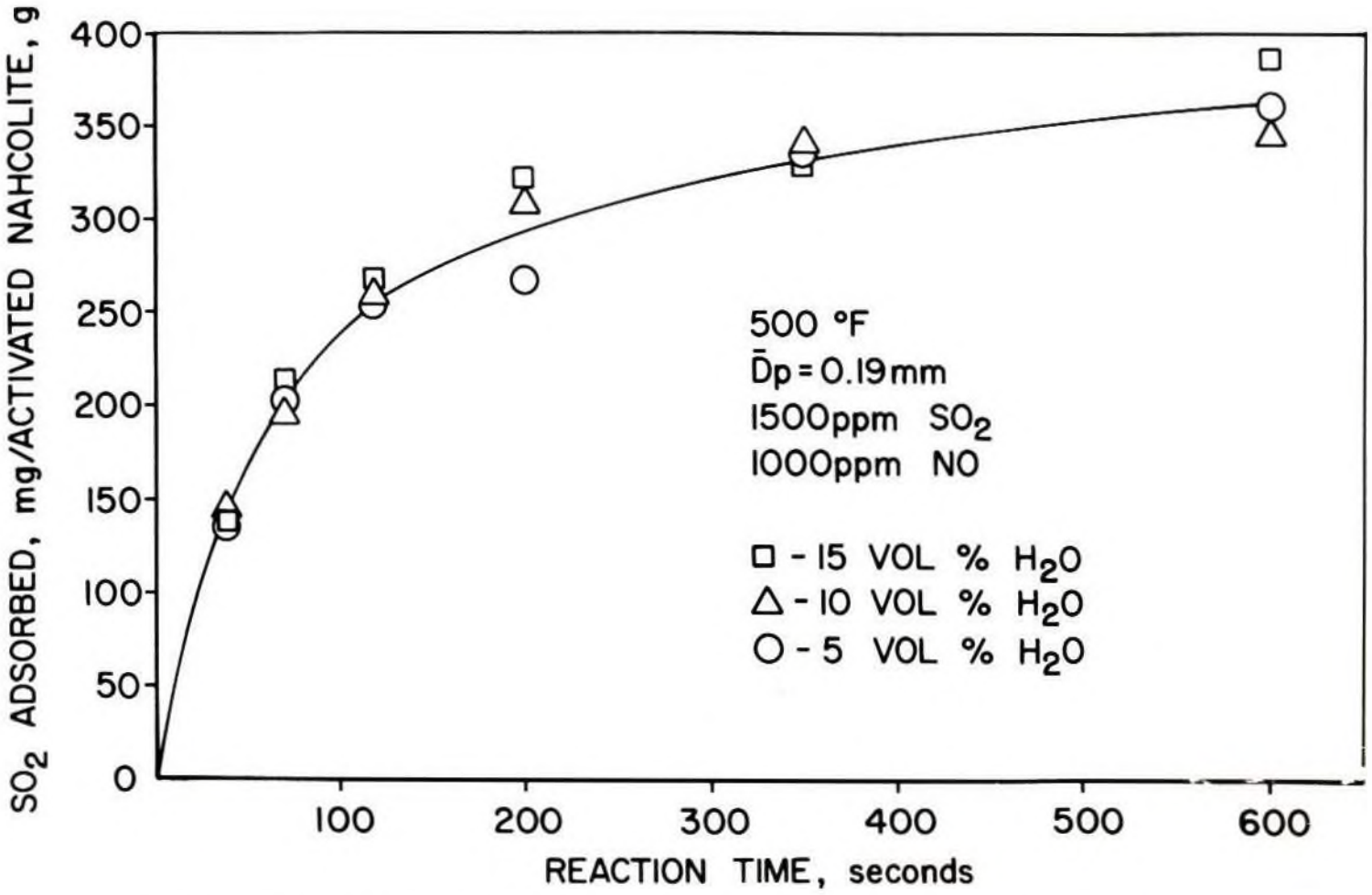

Figure 22.- Effect of flue gas moisture on SO_2 adsorbance.

Effect of Flue Gas SO_2 Concentration

Figure 23 shows the effect of gaseous SO_2 loading on the adsorption of SO_2. At longer reaction times the extent of nahcolite conversion was essentially the same, approximately 75 pct, for each of the SO_2 concentrations tested. This utilization is in close agreement with utilization shown for the 0.19 mm particles under other conditions.

A significant increase in reaction rate was observed as the concentration of SO_2 in the flue gas was increased. The resultant slope of 0.99 for the log of reaction rate versus SO_2 concentration plot, Figure 24, indicates that the reaction of nahcolite with SO_2 is first order with respect to SO_2.

Comparison of Nahcolite and Trona

When compared to nahcolite tested at identical conditions, trona exhibited a much lower reaction rate and utilization as indicated in Figures 25 and 26. As with nahcolite, the reaction rate and utilization of trona increased as the reaction temperature was increased and the particle size decreased. However, at each set of conditions tested the utilization of trona was approximately 50 pct less than that of nahcolite. The only apparent explanation for these results is the significantly lower specific surface area of trona.

Adsorption of NO

As indicated in Figures 27 and 28, only small amounts of NO were adsorbed by nahcolite and trona. The rate of NO adsorption was observed to increase as the reaction temperature decreased. At reaction temperatures of 650° and 750° F no adsorption of NO was detected. The absence of NO

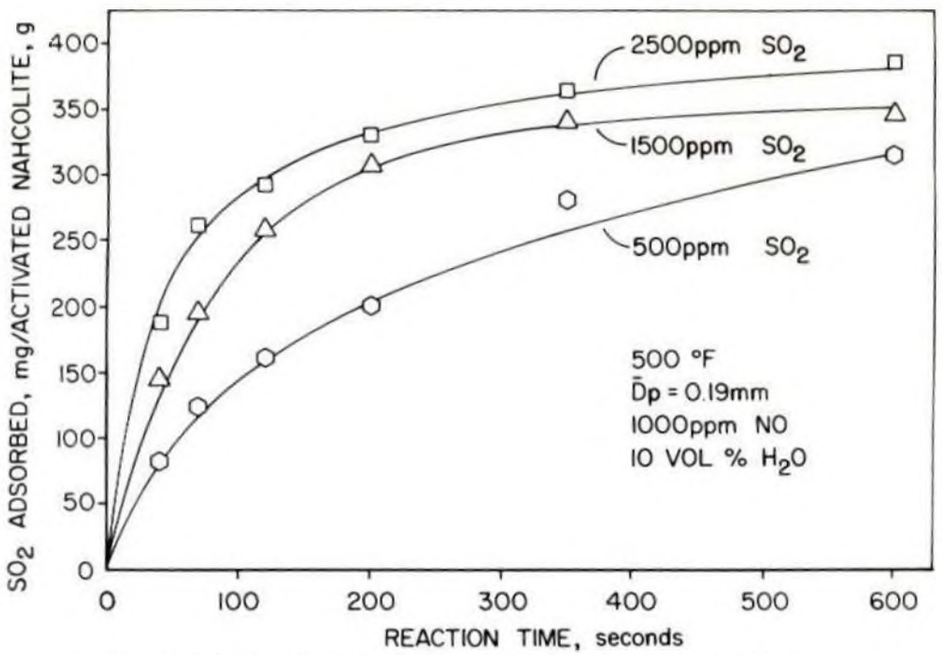

Figure 23.-Sorption of SO_2 at various SO_2 concentrations.

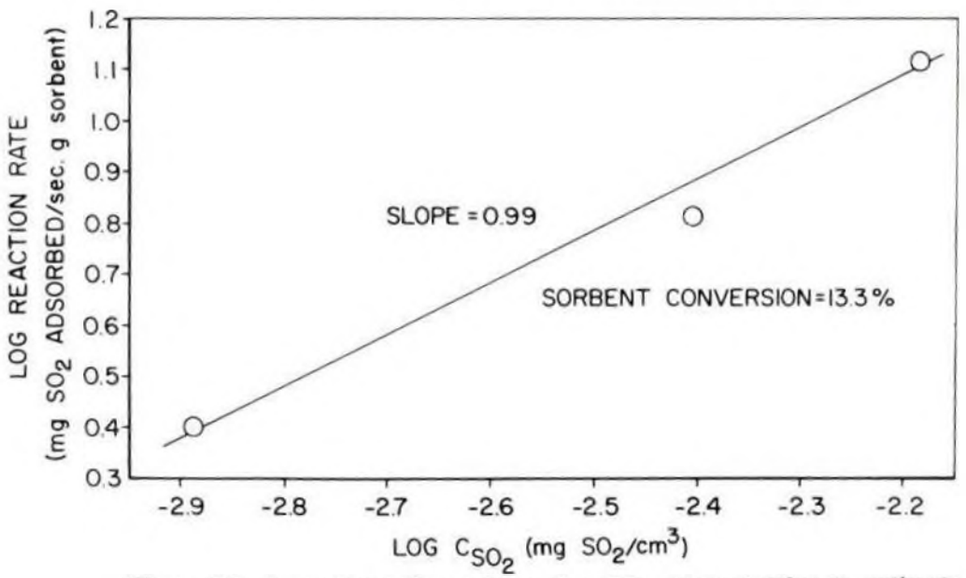

Figure 24.-Log of reaction rate vs. log SO_2 concentration to estimate m.

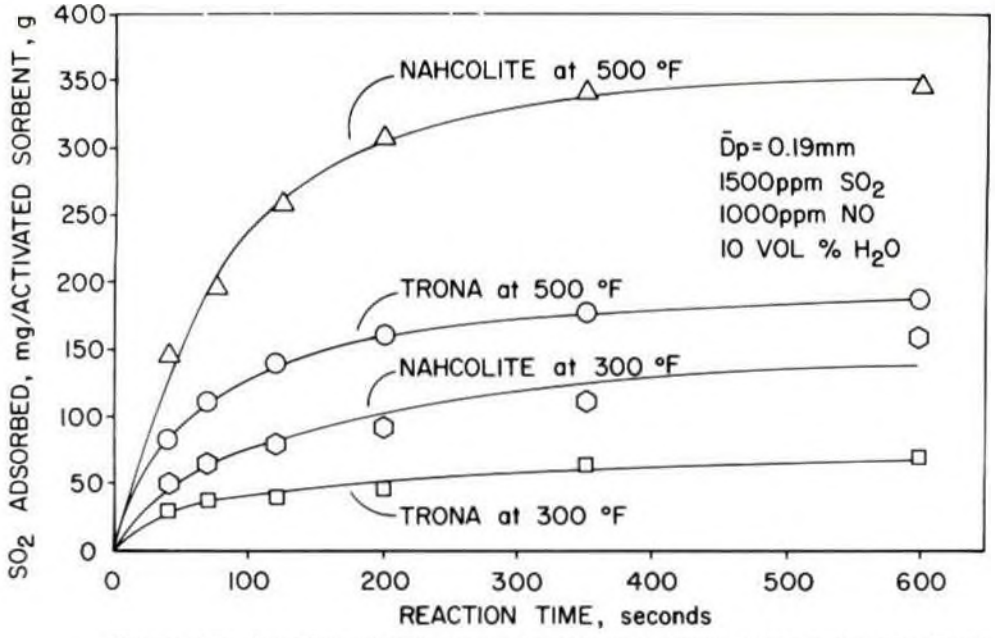

Figure 25.-Sorption of SO_2 on nahcolite and trona at two temperatures.

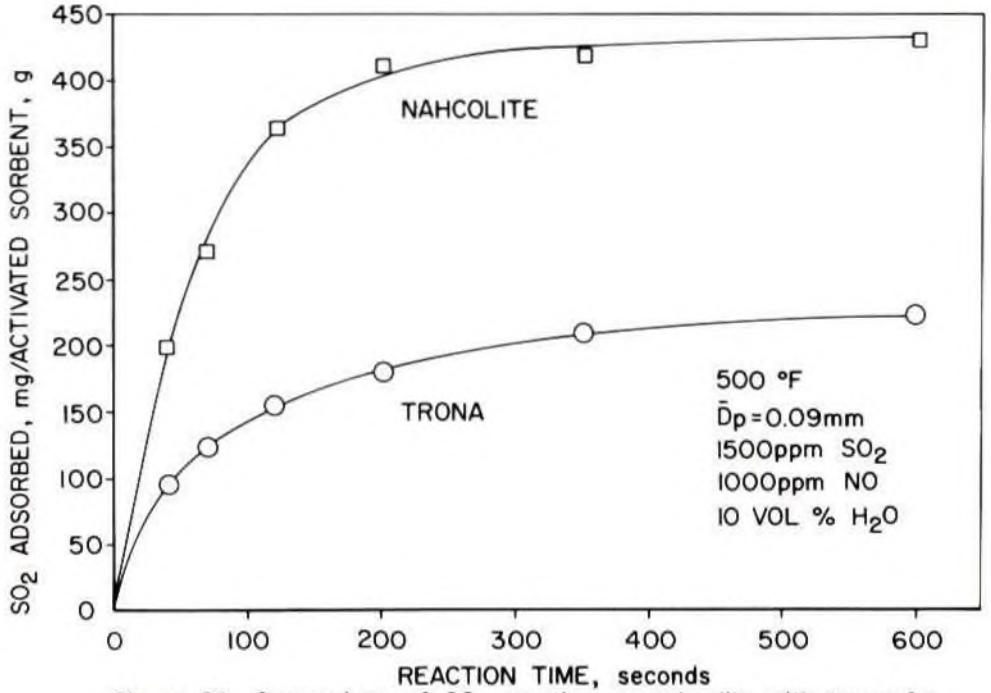

Figure 26.-Comparison of SO_2 sorption on nahcolite with trona for small particles.

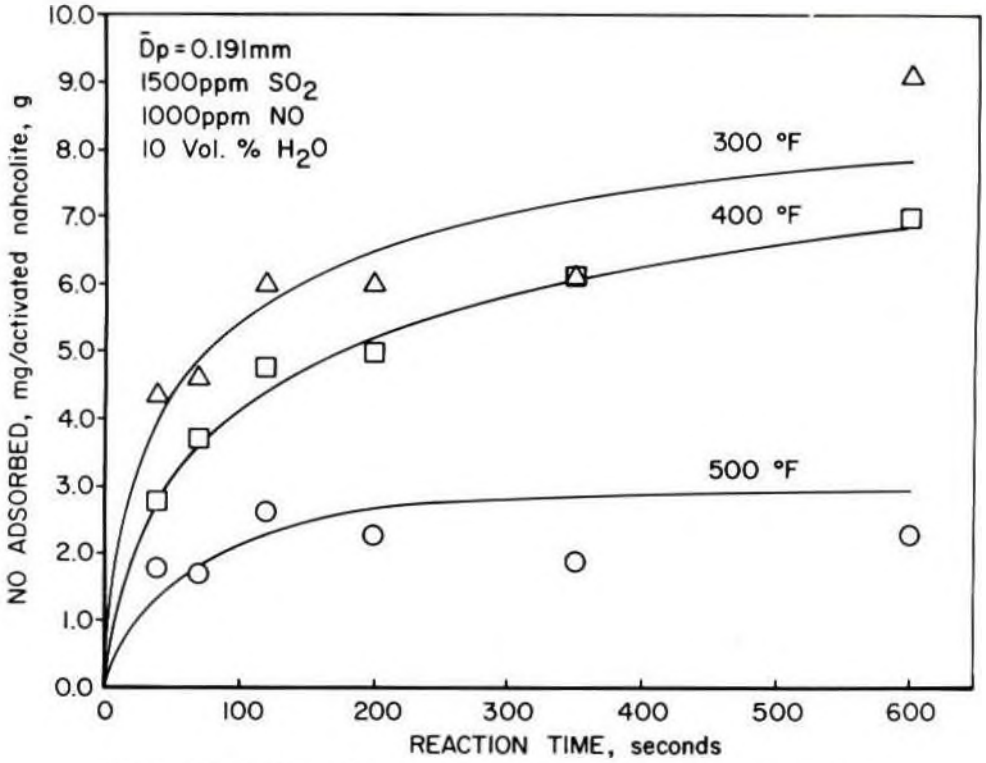

Figure 27.- NO sorption on nahcolite at various temperatures.

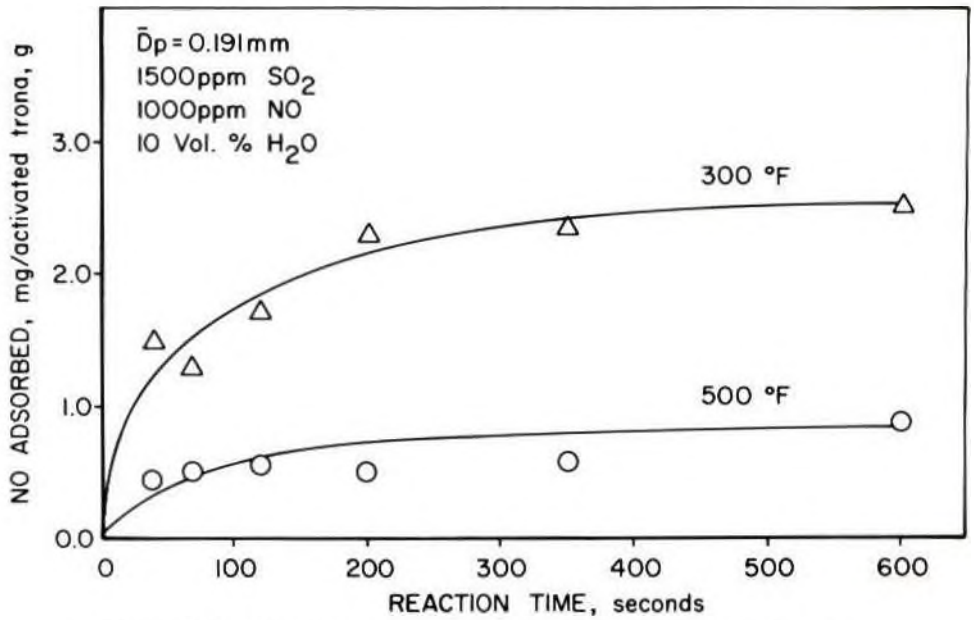

Figure 28.- Adsorption of NO on trona at two temperatures.

adsorption at these temperatures was expected because of the decomposition of both $NaNO_2$ and $NaNO_3$ at temperatures above 600° F.

In analyzing the reacted sorbent, the diazotization method was used for determining $NaNO_2$, and $NaNO_3$ was quantified by specific ion electrode (19). $NaNO_2$ was not present in any of the samples tested and therefore all NO adsorbance numbers presented here are based on the sodium nitrate content of the reacted sorbent.

Rate Controlling Step

Determination of the rate controlling step for the nahcolite-SO_2 reaction was conducted by comparing experimental results with theoretical values predicted by Equations [6], [7], and [8]. For each set of conditions tested, chemical reaction appeared to be rate controlling initially. As the reaction progressed and the surface area covered by adsorbate increased, the reaction resistance due to ash layer diffusion became more significant. Further conversion of the sorbent particles led to recognition of ash layer diffusion as being the rate controlling step. Figure 29 presents a typical comparison of the experimental values with the theroretical curves predicted by Equations [7] and [8].

The nahcolite conversion values at which chemical reaction, ash layer diffusion, or a combination of both were observed to be rate controlling were dependent on particle size and reaction temperature. In general, chemical reaction was the rate controlling step for a larger portion of the conversion in the cases of small particle sizes and decreased temperatures. Estimated conversion value ranges for the stated reaction resistances are given in Table 7.

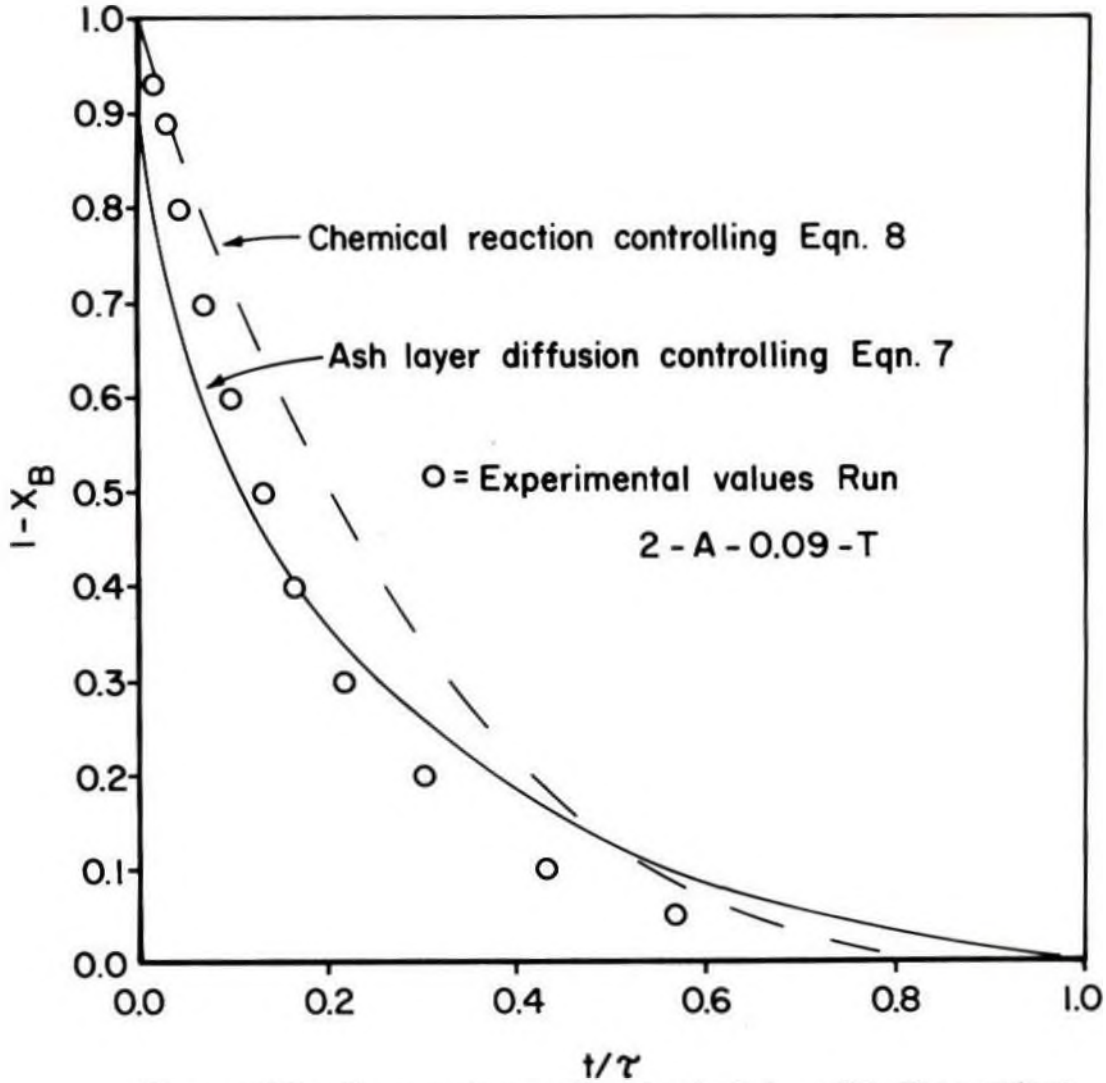

Figure 29. - Comparison of actual data with theoretical curves of two rate controlling steps.

TABLE 7

ESTIMATES OF SORBENT CONVERSION RANGES
UNDER VARIOUS RATE CONTROLLING STEPS

	Fraction of Sorbent Conversion		
Run Number	Chemical reaction	Chemical reaction/ ash layer diffusion	Ash layer diffusion
1-A-300-T	0.00 - 0.06	0.06 - 0.18	0.18-
1-A-400-T	0.00 - 0.07	0.07 - 0.32	0.32-
1-A-500-T	0.00 - 0.06	0.06 - 0.31	0.31-
1-A-650-T	0.00 - 0.04	0.04 - 0.23	0.23-
1-A-750-T	0.00 - 0.06	0.06 - 0.26	0.26-
2-A-.09-T	0.00 - 0.08	0.08 - 0.58	0.58-
2-A-.50-T	0.00 - 0.03	0.03 - 0.18	0.18-
4-A-500-T	0.00 - 0.05	0.05 - 0.40	0.40-
4-A-2500-T	0.00 - 0.05	0.05 - 0.27	0.27-

Overall Rate Expression

Recognizing that both chemical reaction and diffusion through the 'ash' layer presented significant resistance to the overall reaction, Equations [10] and [11] were combined to describe the overall reaction rate giving (13):

$$\frac{dN_A}{dt} = \frac{4\pi D C_{Ag}}{\left(\frac{1}{r_c} - \frac{1}{R}\right)} + 4\pi k_s C_{Ag} r_c^2 \qquad [16]$$

Substituting for r_c as given by Equation [13], adding a term for particle weight, and rearranging gives the following expression:

$$\frac{dN'_A}{dt} = \frac{4\pi R C'_{Ag}}{W} \left[\frac{D(1-X_B)^{1/3}}{1-(1-X_B)^{1/3}} + k_s R(1-X_B)^{2/3}\right] \qquad [17]$$

where, N'_A = SO_2 adsorbed, mg/g activated sorbent

C'_{Ag} = gaseous SO_2 concentration, mg/cm^3

W = weight of a single particle, g

Combining terms to obtain an overall rate expression is not an elaborate method of expressing coupled processes, but it is considered adequate for the data presented here. The only unknown variables in Equation [17], D and k_s, were then solved for simultaneously by a computer program utilizing a least squares fit from ten sorbent conversion-reaction rate data points for each set of kinetic runs. The computer program used for this determination was the U.S. Bureau of Standards OMNITAB Program.

Figure 30 presents a comparison of the reaction rate predicted by Equation [17] with values determined by Equation [15] for a typical kinetic run. Values of D and k_s for other kinetic runs with nahcolite are given in Table 8.

TABLE 8

DIFFUSION AND RATE CONSTANT VALUES
OBTAINED BY COMPUTER SOLUTION OF EQUATION [17]

Run Number	Diffusivity $cm^2/sec \times 10^{-3}$	Rate constant, cm/sec	Multiple correlation squared
1-A-300-T	0.52	- 0.14	0.96
1-A-400-T	1.79	2.48	.93
1-A-500-T	2.58	5.74	.87
1-A-650-T	5.44	4.32	.93
1-A-750-T	3.27	3.83	.93
2-A-.50-T	7.81	- .34	.95
2-A-.09-T	1.86	2.06	.97
4-A-500-T	4.02	3.58	.92
4-A-2500-T	3.18	5.25	.92

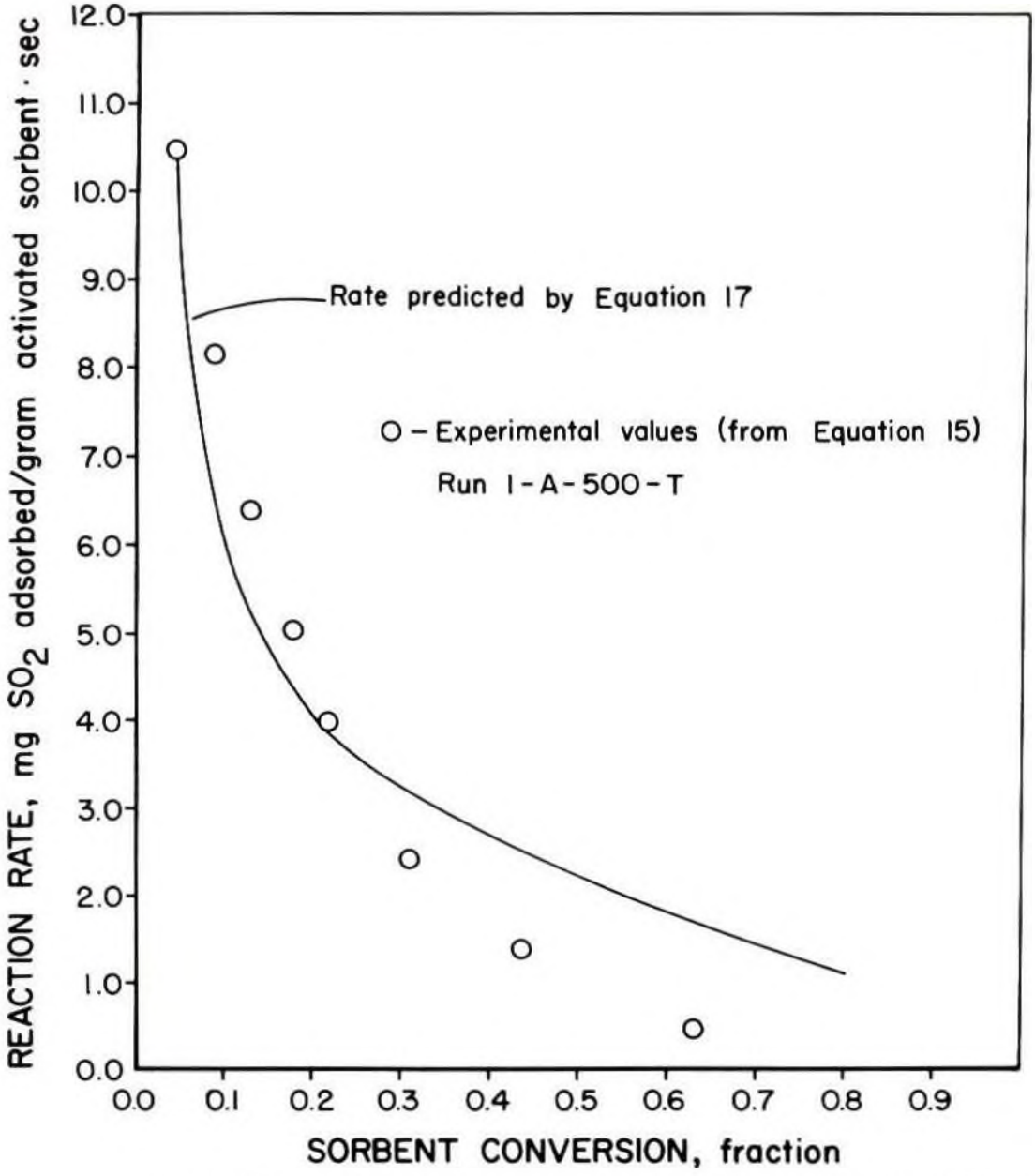

Figure 30. – Comparison of rate predicted by Equation 17 with experimental values.

It should be noted that values given in Table 8 are the best fit of a mathematical equation. Since no restrictions were placed on the coefficients, it is possible that a coefficient may have been under or over-emphasized during computations, resulting in a slightly negative rate value.

As shown in Table 8, the values for diffusivity and reaction rate constants increased with reaction temperature as expected with the exception of tests at 750° F. The lower diffusivity and rate constant at this temperature is thought to be due to the smaller specific surface area of nahcolite at 750° F.

Values of diffusivity and rate constants were expected to remain relatively constant for tests of varying particle size and SO_2 concentration. Although values varied considerably for such tests, the most notable variation occurred in diffusivity values for varying particle sizes.

The higher diffusivity indicated in Table 8 for large particle sizes can be attributed to more extensive pore development in the larger particles. Based on the surface area of a spherical particle, the specific surface area per gram of a 0.50 mm diameter particle should be approximately 80 pct less than that of 0.09 mm particles. However, as indicated in Table 9, Appendix A, the specific surface area of 0.50 mm diameter nahcolite particles is only 21 pct less than the specific surface area of 0.09 mm diameter nahcolite particles. This suggests greater pore development in the larger particles thereby reducing the resistance to diffusion. The only explanation for this increased porosity is that the larger particles may have been subject to greater thermal and pressure stresses during activation.

APPLICATION TO POWER PLANT FGD

The results of this study indicate nahcolite to be a viable sorbent of SO_2. As a dry sorbent, nahcolite could perhaps be best used in a FGD system utilizing a baghouse. The nahcolite could be injected into the hot flue gas stream near the air preheater section at a site where the gas temperature is 600-700° F. Injection at these temperatures would result in high reaction rates and yet not cause extensive sintering of the nahcolite. The partially reacted nahcolite would then be collected downstream in a baghouse.

The baghouse would remove other particulate matter along with nahcolite from the flue gas and act as a gas-solid contacting device for continued nahcolite-SO_2 reaction. Based on results of this study more favorable utilization and reactivity would be realized by injecting nahcolite particles of -100 Tyler mesh and by operating the baghouse at temperatures above 300° F.

Although nahcolite appears to be a feasible sorbent for 'dry' FGD methods, its use in a commercial process remains in doubt. Use of nahcolite will firstly depend on nahcolite becoming commercially available. Secondly, should nahcolite become available, its cost must be low enough such that the 'dry' process will be economically favorable.

CONCLUSIONS

Due to sufficient utilization and reaction rate of nahcolite, it appears that nahcolite would be an effective sorbent for use in 'dry' FGD systems. The most favorable utilizations and reaction rates for the nahcolite-SO_2 reaction were noted at temperatures of 400-650° F and sorbent particle sizes of less than 0.19 mm in diameter. Trona demonstrated considerable capability for SO_2 removal also, but utilization and reaction rate were far less favorable. Both nahcolite and trona adsorbed only small quantities of NO, amounting to less than 2.5 pct of the sorbent utilization possible.

Based on test results and observations, other conclusions of this investigation are:

1. Reaction Temperature - The rate of reaction with SO_2 increases with temperature for temperatures up to 650° F. For temperatures above 650° F the reaction rate decreases because of sorbent sintering.
2. Particle Size - The reaction rate of sorbent with SO_2 and sorbent utilization increases rapidly as the particle size decreases.
3. SO_2 Loading - The reaction rate of nahcolite with SO_2 is directly proportional to the gaseous SO_2 concentration.

4. Flue Gas Moisture - At a reaction temperature of 500° F varying the volume percentage of moisture in the flue gas from 5 to 15 pct has no significant effect on reaction rate or utilization.

5. Rate - Controlling Step - Under the conditions tested, chemical reaction was the rate controlling step only for initial portions of the reaction. The remaining majority of the reaction period was rate controlled by reactant diffusion through the ash layer.

6. NO Adsorption - Trona adsorbed less NO than nahcolite. For both nahcolite and trona the rate of NO adsorption was very low and decreased as the reaction temperature increased.

7. Sorbent Activation - The surface area developed by thermal activation increases with activation temperature. However, extended heating of nahcolite at temperature above 650° F causes reduced surface area.

8. Activation Energy - Based on data from three reaction temperatures the energy of activation for the nahcolite-SO_2 reaction was calculated to be 10,470 cal/g mole.

9. Overall Rate Expression - By combining mathematical expressions for the rate of gas diffusion in a solid particle and for the chemical reaction of a particle, a rate expression was obtained that fit experimental values. Diffusivity was determined to be 0.0026 cm^2/sec and the rate constant was 5.74 cm/sec for the reaction of nahcolite with SO_2 at 500° F.

RECOMMENDATIONS

The investigation of utilizing sorbents for 'dry' FGD is not complete. Recommendations for further study are as follows:

1. Since in some applications it may not be possible to operate at determined optimum conditions, additional experimentation should be conducted at lower reaction temperatures and with larger sorbent particle sizes.
2. The effect of flue gas moisture at low reaction temperatures should be investigated.
3. The adsorption of NO by nahcolite and trona in the presence of higher O_2 concentrations should be studied. A similar study using NO_2 as the adsorbate would also be of interest.
4. Expand the activation study of nahcolite and trona to include high temperature activation at extremely low residence times of 3 to 4 seconds. (It will be necessary to design a special apparatus for this study.)
5. Potential sorbent materials such as potash, chars derived from Western coals, and Western fly ashes should be submitted to SO_2 adsorption screening tests.
6. The experimental apparatus used in this study could be modified to allow sorbent placement into the reactor after the reactor has reached the selected reaction temperature. This modification would allow materials, which had not undergone a physical or chemical change prior to reactor introduction, to be studied.

APPENDICES

APPENDIX A

TABLE 9

COMPOSITION AND PHYSICAL CHARACTERISTICS OF TEST MATERIALS

	Nahcolite						Trona			
	$\bar{D}p$ = 0.50 mm		$\bar{D}p$ = 0.19 mm		$\bar{D}p$ = 0.09 mm		$\bar{D}p$ = 0.19 mm		$\bar{D}p$ = 0.09 mm	
	Raw	Activated	Raw	Activated	Raw	Activated	Raw	Activated	Raw	Activated
Composition, wt pct:										
Na_2CO_3.....	9.8	71.0	6.5	74.8	8.2	74.2	41.9	83.4	41.2	83.7
$NaHCO_3$.....	61.1	.2	71.6	1.1	69.0	.6	29.6	.0	32.0	.1
$CaCO_3$.....	2.0	3.0	1.7	2.5	1.7	2.5	2.5	3.4	2.4	3.3
$MgCO_3$.....	1.6	2.3	1.1	1.7	1.4	2.1	1.2	1.6	1.2	1.7
Na_2SO_4.....	1.6	2.3	1.6	2.3	1.9	2.8	.5	.7	.5	.7
Water insolubles[a]..	16.8	23.7	13.3	17.6	13.3	17.9	8.0	11.0	7.7	10.7
H_2O[b].....	7.1	.0	4.2	.0	4.5	.0	16.3	.0	16.0	.0
Wt. pct change on activation.....	-32.7		-32.5		-32.8		-27.4		-28.0	
Surface area,[c] m^2/g..	6.0		6.8		7.6		3.2		4.2	
Bulk density, g/cm^3..	.72		.67		.67		.80		.73	
True density,[d] g/cm^3.	2.51		2.51		2.44		2.50		2.51	

a - includes organics
b - by difference
c - as determined on the Quantachrome Monosorb Surface Area Analyzer
d - as determined on the Micromeritics Pycnometer Model 1302

APPENDIX B

Calculation of SO_2 and NO Adsorption

The amount of SO_2 adsorbed was based on the sulfur analysis reported by X-ray fluorescence. Values were calculated as follows:

$$\frac{\text{mg } SO_2 \text{ adsorbed}}{\text{g activated sorbent}} = \frac{\left(\frac{\text{wt \% } SO_4}{100\%} \text{ gram}\right)_r - \left(\frac{\text{wt \% } SO_4}{100\%} \text{ gram}\right)_a}{(\text{gram})_a \left(\frac{\text{gram}}{1000 \text{ mg}}\right)\left(\frac{96 \text{ g } SO_4}{64 \text{ g } SO_2}\right)}$$

The subscripts, r and a, indicate reacted and activated sorbent respectively.

Based on results of the nitrate analysis, the amount of NO adsorbed was calculated in a similar manner.

$$\frac{\text{mg NO adsorbed}}{\text{g activated sorbent}} = \frac{\left(\frac{\text{wt \% } NO_3}{100\%} \text{ gram}\right)_r - \left(\frac{\text{wt \% } NO_3}{100\%} \text{ gram}\right)_a}{(\text{gram})_a \left(\frac{\text{gram}}{1000 \text{ mg}}\right)\left(\frac{62 \text{ g } NO_3}{30 \text{ g NO}}\right)}$$

Flue Gas Flow Rate and Water Vapor Percentage Calculations

The dry flue gas flow rate was calculated by the following equation given by McCabe and Smith (20).

$$\dot{m} = \frac{C_o \; S_o}{\sqrt{(1-\beta^4)}} \; \left((2g_c(P_a - P_b)\rho_a)^{1/2}\right)$$

where, $\dot{m}$ = mass flow rate, lb/sec

C_o = orifice coefficient, dimensionless (experimentally determined to be 0.63)

S_o = cross sectional area of orifice, ft^2 (determined to be 0.00136 ft^2)

β = orifice diameter/pipe diameter, dimensionless

$$\left(\frac{0.5 \text{ in}}{0.75 \text{ in}}\right) = 0.667$$

g_c = Newton's -law proportionality factor,

$$32.17 \text{ ft lb/lb}_f(\text{sec}^2)$$

$P_a - P_b$ = orifice differential pressure, lb_f/ft^2

ρ_a = gas density upstream of orifice, lb/ft^3

The volumetric flow rate was then calculated at 1 atm and 32° F as follows:

$$V_G(\text{dry}) = \dot{m}\left(\frac{359 \text{ ft}^3}{\text{lb mol}}\right)\left(\frac{1}{Mw}\right)$$

where, V_G = volumetric flow rate, ft^3/sec

Mw = average molecular weight of gas, lb/lb mol

The volume percent moisture of the gas leaving the water bath was determined by noting the vapor pressure of H_2O and assuming that mole percent H_2O is equivalent to volume percent H_2O. The volume percent H_2O was calculated as

$$\text{vol. \% } H_2O = \frac{P_{H_2O,T}}{P_t}(100\%)$$

where, $P_{H_2O,T}$ = vapor pressure of water at water bath temperature of T, psia

P_t = water bath pressure, psia

The volumetric flow rate of the simulate flue gas including moisture was then computed as follows:

$$V_G(\text{wet}) = \frac{V_G(\text{dry})}{1.0 - (\frac{\text{vol. \% } H_2O}{100})}$$

Calculation of Activation Energy

Calculation of the activation energy for the nahcolite-SO_2 reaction was performed using the expression for activation energy given by Fogler (21). The expression, derived from the Arrhenius equation, is given as

$$E = \frac{2.3R\log (\frac{k1}{k_2})}{(\frac{1}{T_2} - \frac{1}{T_1})}$$

where, E = activation energy, cal/g mol

R = gas constant, 1.987 cal/g mol °K

k = reaction rate constant, cm/sec

T = reaction temperature, °K

Noting that the reaction rate is directly proportional to the rate constant, the activation energy was calculated from the following values taken from Figure 18.

at T_1 = 434.8° K, the reaction rate = 0.931 mg SO_2/g sorbent · sec

and at T_2 = 540.5° K, the reaction rate = 9.99 mg SO_2/g sorbent · sec.

Substituting the ratio of reaction rates for the ratio of reaction rate constants then gives

$$E = \frac{(2.3)\ (1.987 \text{ cal/g mol °K})\ \log \frac{0.931}{9.99}}{(\frac{1}{540.5° \text{ K}} - \frac{1}{434.8° \text{ K}})} = 10{,}470 \text{ cal/g mol}$$

Reproducibility

In order to determine the variance and confidence interval of the experimental tests, five replicates of Run 1-A-500-120 were conducted. The variance was calculated as

$$s^2 = \frac{\Sigma (\chi_i - \bar{\chi})^2}{N - 1}$$

and the confidence interval of the average for five tests by,

$$\pm t_{(\alpha/2)(F)} \sqrt{\frac{s^2}{N}}$$

where χ_i is the observed value, $\bar{\chi}$ the mean value, N the number of tests, α the confidence level, and F the degrees of freedom (22). Based on the values, α = 0.95, F = 4, and t = 2.776, 95 pct of the average of the replicated values should be within $\pm$ 4 pct.

TABLE 10

VALUES OF CONSTANTS FOR EQUATION [14] AS DETERMINED BY LEAST SQUARES LINEAR REGRESSION[a]

Test Number	a	b	Regression coefficient r^2
1-A-300-T	130.38	41.97	0.82
1-A-400-T	319.49	46.83	.93
1-A-500-T	366.35	38.40	.98
1-A-650-T	358.27	30.61	.99
1-A-750-T	348.65	34.22	.94
2-A-0.09-T	184.75	43.23	.98
2-A-0.50-T	467.78	34.46	.99
3-A-5-T	363.15	40.53	.98
3-A-15-T	392.85	41.97	.99
4-A-500-T	297.85	55.36	.93
4-A-2500-T	393.10	29.52	.99
1-B-300-T	63.80	31.82	.80
1-B-500-T	194.20	34.00	.98
2-B-0.09-T	222.10	35.87	.97

a - computed by Hewlett-Packard HP-97 Standard Pac Program SD-03A

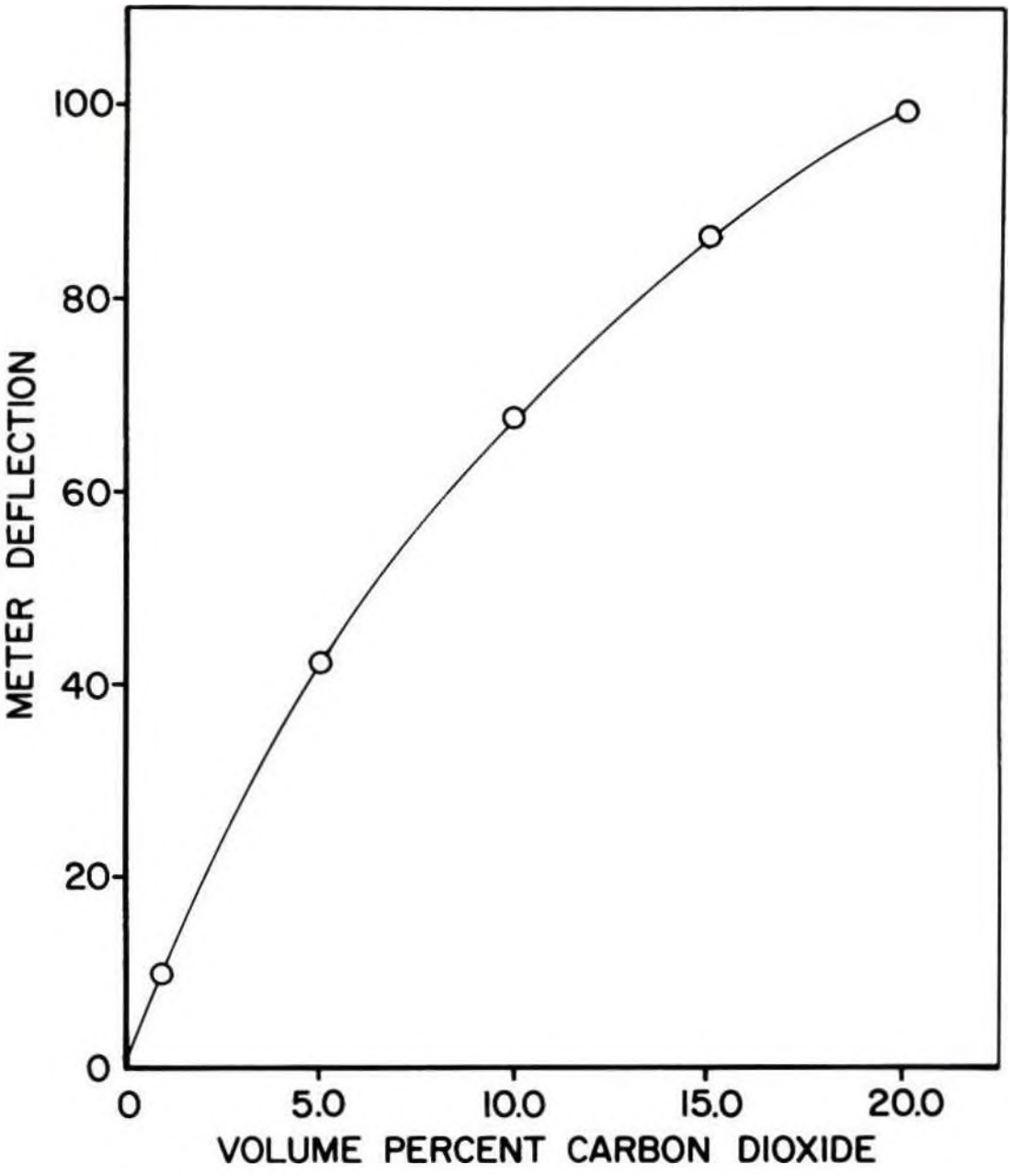

Figure 31. – Calibration curve for Beckman Model 864 CO_2 Analyzer.

TABLE 11

TEST RESULTS OF SULFUR DIOXIDE AND NITRIC OXIDE ADSORPTION

Run No.	Reactor No.	Reactor Temp., °F	Water Bath		Flue Gas Flow				Flue Gas Composition						Sorbent In	Sorbent Out		
			Press., psia	Temp., °F	Orifice Inlet Press., psia	Orifice Diff. Press. in H_2O	Orifice Temp., °F	Flow Rate scfm(wet)	CO_2, volt	O_2, volt	N_2, volt	H_2O, volt	NO, ppm	SO_2, ppm	Wt., grams	Wt., grams	SO_2 Adsorbed, mg	NO Adsnr mg
1-A-300-40	2	300	26.7	136	29.4	3.6	53	10.5	13.5	4.5	72.2	9.7	1000	1500	3.00	3.11	153.6	13.1
1-A-300-70	2	300	26.7	136	29.5	3.6	53	10.5	13.5	4.5	72.2	9.7	1000	1500	3.01	3.12	195.7	13.8
1-A-300-120	3	300	26.7	136	29.3	3.7	53	10.6	13.5	4.5	72.2	9.7	1000	1500	3.01	3.16	240.5	18.3
1-A-300-200	4	300	26.7	136	29.4	3.6	53	10.5	13.5	4.5	72.2	9.7	1000	1500	3.00	3.17	274.5	18.0
1-A-300-350	4	300	26.7	136	29.5	3.6	52	10.5	13.5	4.5	72.2	9.7	1000	1500	3.00	3.21	334.5	18.3
1-A-300-600	3	300	26.7	136	29.5	3.6	53	10.5	13.5	4.5	72.2	9.7	1000	1500	3.00	3.30	493.5	27.6
1-A-400-40	4	400	27.7	140	29.7	3.5	49	10.5	13.5	4.5	71.7	10.3	1000	1500	3.00	3.21	417.7	8.4
1-A-400-70	3	400	27.7	140	29.7	3.5	49	10.5	13.5	4.5	71.7	10.3	1000	1500	3.01	3.23	434.2	11.1
1-A-400-120	3	400	27.7	140	29.9	3.5	52	10.5	13.5	4.5	71.7	10.3	1000	1500	3.00	3.30	557.1	14.4
1-A-400-200	2	400	27.7	140	30.0	3.4	51	10.4	13.5	4.5	71.7	10.3	1000	1500	3.01	3.43	779.9	15.0
1-A-400-350	3	400	27.7	140	30.1	3.5	52	10.6	13.5	4.5	71.7	10.3	1000	1500	3.01	3.51	895.8	18.3
1-A-400-600	2	400	27.7	140	30.2	3.5	52	10.6	13.5	4.5	71.7	10.3	1000	1500	3.01	3.56	965.6	21.1
1-A-500-40	3	500	30.0	142	32.3	3.4	47	10.8	13.5	4.5	71.8	10.2	1000	1500	3.05	3.28	446.2	5.4
1-A-500-70	4	500	30.0	142	32.2	3.3	48	10.6	13.5	4.5	71.8	10.2	1000	1500	3.02	3.30	592.2	5.1
1-A-500-120	4	500	30.0	142	32.3	3.3	49	10.6	13.5	4.5	71.8	10.2	1000	1500	3.01	3.44	779.9	8.1
1-A-500-200	2	500	30.0	142	32.3	3.4	48	10.7	13.5	4.5	71.8	10.2	1000	1500	3.05	3.59	941.8	6.9
1-A-500-350	3	500	30.0	142	32.2	3.4	48	10.8	13.5	4.5	71.8	10.2	1000	1500	3.07	3.60	906.0	5.7
1-A-500-600	2	500	30.0	142	32.3	3.3	47	10.7	13.5	4.5	71.8	10.2	1000	1500	3.09	3.71	1058.6	6.9
1-A-650-40	3	650	31.7	143	33.8	3.1	56	10.4	13.5	4.5	72.7	9.3	1000	1500	3.01	3.23	490.0	____
1-A-650-70	2	650	32.8	143	34.6	3.0	57	10.3	13.5	4.5	72.1	9.9	1000	1500	3.00	3.37	728.2	____
1-A-650-120	4	650	33.7	143	35.7	2.8	57	10.1	13.5	4.5	72.4	9.6	1000	1500	3.00	3.42	826.4	____
1-A-650-200	4	650	33.7	143	35.8	2.9	57	10.2	13.5	4.5	72.7	9.3	1000	1500	3.02	3.51	916.6	____
1-A-650-350	2	650	32.8	143	34.6	3.0	57	10.3	13.5	4.5	72.1	9.9	1000	1500	3.00	3.54	995.3	____
1-A-650-600	3	650	31.7	143	33.8	3.1	56	10.4	13.5	4.5	72.4	9.6	1000	1500	3.04	3.55	1000.4	____
1-A-750-40	4	750	34.6	144	36.8	2.8	54	10.3	13.5	4.5	78.8	9.3	1000	1500	3.01	3.16	432.9	_
1-A-750-70	3	750	34.3	144	35.7	2.9	50	10.3	13.5	4.5	72.7	9.3	1000	1500	3.00	3.32	690.2	_ _
1-A-750-120	2	750	34.7	144	36.7	3.0	54	10.7	13.5	4.5	72.8	9.2	1000	1500	3.00	3.37	801.6	____
1-A-750-200	3	750	34.7	144	36.7	3.1	54	10.8	13.5	4.5	72.8	9.2	1000	1500	3.00	3.38	810.2	____
1-A-750-350	2	750	34.5	144	36.2	2.8	52	10.2	13.5	4.5	72.7	9.3	1000	1500	3.00	3.44	875.8	____
1-A-750-600	4	750	34.5	144	36.7	2.8	50	10.2	13.5	4.5	72.7	9.3	1000	1500	3.01	3.66	1097.3	____
2-A-.50-40	3	500	28.7	141	30.6	3.3	48	10.3	13.5	4.5	71.7	10.3	1000	1500	3.01	3.11	199.3	N/A
2-A-.50-70	4	500	28.5	141	30.2	3.4	48	10.4	13.5	4.5	71.7	10.3	1000	1500	3.01	3.16	276.6	N/A

TABLE 11 (con't)

Run No.	Reactor No.	Reactor Temp., °F	Water Bath Press., psia	Water Bath Temp., °F	Flue Gas Flow Orifice Inlet Press., psia	Flue Gas Flow Orifice Diff. Press., in H_2O	Flue Gas Flow Orifice Temp., °F	Flue Gas Flow Flow Rate scfm(wet)	Flue Gas Composition CO_2, volt	Flue Gas Composition O_2, volt	Flue Gas Composition N_2, volt	Flue Gas Composition H_2O, volt	Flue Gas Composition NO, ppm	Flue Gas Composition SO_2, ppm	Sorbent In Wt., grams	Sorbent Out Wt., grams	Sorbent Out SO_2 Adsorbed, mg	Sorbent Out NO Adsorbed mg
2-A-.50-120	2	500	28.6	141	30.2	3.4	47	10.4	13.5	4.5	71.7	10.3	1000	1500	3.01	3.21	371.5	N/A
2-A-.50-200	3	500	28.5	141	30.3	3.3	47	10.3	13.5	4.5	71.7	10.3	1000	1500	3.00	3.25	435.4	N/A
2-A-.50-350	4	500	28.7	141	30.7	3.2	48	10.2	13.5	4.5	71.7	10.3	1000	1500	3.01	3.30	516.2	N/A
2-A-.50-600	2	500	28.7	141	30.6	3.3	47	10.4	13.5	4.5	71.7	10.3	1000	1500	3.01	3.33	540.9	N/A
2-A-.09-40	3	500	31.7	142	33.7	3.0	47	10.3	13.5	4.5	72.4	9.6	1000	1500	3.00	3.35	600.0	N/A
2-A-.09-70	4	500	30.7	142	32.7	3.2	47	10.5	13.5	4.5	72.1	9.9	1000	1500	3.00	3.48	819.0	N/A
2-A-.09-120	2	500	32.0	143	34.2	3.0	47	10.3	13.5	4.5	72.3	9.7	1000	1500	3.00	3.63	1080.1	N/A
2-A-.09-200	3	500	31.7	142	33.7	3.0	46	10.4	13.5	4.5	72.4	9.6	1000	1500	3.00	3.70	1207.2	N/A
2-A-.09-350	4	500	30.5	142	32.7	3.2	47	10.5	13.5	4.5	72.0	10.0	1000	1500	3.00	3.73	1251.5	N/A
2-A-.09-600	2	500	32.0	143	34.2	3.0	46	10.3	13.5	4.5	72.3	9.7	1000	1500	3.00	3.76	1312.2	N/A
3-A-5-40	2	500	30.0	115	32.0	3.6	53	10.4	13.5	4.5	77.0	5.0	1000	1500	3.00	3.23	415.8	N/A
3-A-5-70	2	500	30.1	115	32.5	3.6	54	10.5	13.5	4.5	77.0	5.0	1000	1500	3.00	3.33	601.2	N/A
3-A-5-120	3	500	30.0	115	32.0	3.7	55	10.5	13.5	4.5	77.0	5.0	1000	1500	3.00	3.43	767.7	N/A
3-A-5-200	3	500	29.7	115	31.7	3.7	52	10.5	13.5	4.5	77.0	5.0	1000	1500	3.00	3.46	806.0	N/A
3-A-5-350	3	500	30.0	115	32.1	3.7	54	10.5	13.5	4.5	77.0	5.0	1000	1500	3.00	3.56	1016.8	N/A
3-A-5-600	2	500	30.0	115	32.2	3.6	56	10.4	13.5	4.5	77.0	5.0	1000	1500	3.00	3.60	1080.6	N/A
3-A-15-40	3	500	29.4	155	31.2	3.0	56	10.4	12.5	4.5	66.7	14.3	1000	1500	3.00	3.23	419.2	N/A
3-A-15-70	2	500	29.6	156	31.6	3.0	56	10.4	12.5	4.5	66.8	14.2	1000	1500	3.00	3.36	636.5	N/A
3-A-15-120	3	500	29.4	155	31.2	3.0	57	10.4	12.5	4.5	66.7	14.3	1000	1500	3.00	3.44	813.2	N/A
3-A-15-200	2	500	29.5	155	31.5	3.0	55	10.3	12.5	4.5	66.7	14.2	1000	1500	3.00	3.54	974.7	N/A
3-A-15-350	2	500	29.5	155	31.5	3.0	56	10.3	12.5	4.5	66.8	14.2	1000	1500	3.00	3.57	993.3	N/A
3-A-15-600	3	500	29.5	155	31.2	3.0	56	10.3	12.5	4.5	66.8	14.5	1000	1500	3.00	3.62	1161.7	N/A
4-A-500-40	2	500	29.6	141	31.2	3.3	54	10.4	13.5	4.5	72.0	10.0	1000	500	3.00	3.15	247.7	N/A
4-A-500-70	3	500	29.0	141	30.7	3.4	59	10.4	13.5	4.5	71.8	10.2	1000	500	3.00	3.20	373.2	N/A
4-A-500-120	2	500	29.6	141	31.2	3.4	55	10.5	13.5	4.5	72.0	10.0	1000	500	3.00	3.26	483.4	N/A
4-A-500-200	3	500	29.1	141	30.7	3.4	55	10.5	13.5	4.5	71.9	10.1	1000	500	3.00	3.33	602.2	N/A
4-A-500-350	2	500	29.7	141	31.2	3.3	58	10.3	13.5	4.5	72.1	9.9	1000	500	3.00	3.49	846.6	N/A
4-A-500-600	3	500	29.1	141	31.1	3.4	56	10.5	13.5	4.5	71.9	10.1	1000	500	3.00	3.51	946.5	N/A
4-A-2500-40	3	500	29.0	141	30.7	3.4	51	10.5	13.5	4.5	71.8	10.2	1000	2500	3.00	3.30	566.3	N/A
4-A-2500-70	2	500	30.0	141	31.9	3.3	54	10.5	13.5	4.5	72.2	9.8	1000	2500	3.00	3.43	720.5	N/A
4-A-2500-120	3	500	29.0	140	30.8	3.4	50	10.5	13.5	4.5	72.2	9.8	1000	2500	3.00	3.46	885.2	N/A
4-A-2500-200	2	500	29.5	141	31.7	3.3	53	10.5	13.5	4.5	72.0	10.0	1000	2500	3.00	3.56	993.0	N/A

TABLE 11 (con't)

Run No.	Reactor No.	Reactor Temp., °F	Water Bath Press., psia	Water Bath Temp., °F	Flue Gas Flow: Orifice Inlet Press., psia	Flue Gas Flow: Orifice Diff. Press., in H_2O	Flue Gas Flow: Orifice Temp., °F	Flue Gas Flow: Flow Rate scfm(wet)	Flue Gas Composition: CO_2, vol%	O_2, vol%	N_2, vol%	H_2O, vol%	NO, ppm	SO_2, ppm	Sorbent In: Wt., grams	Wt., grams	Sorbent Out: SO_2 Adsorbed, mg	NO Adsorbed, mg
4-A-2500-350	2	500	30.0	141	31.9	3.3	47	10.5	13.5	4.5	72.2	9.8	1000	2500	3.00	3.62	1095.6	N/A
4-A-2500-600	3	500	29.5	141	31.0	3.3	54	10.5	13.5	4.5	72.0	10.0	1000	2500	3.00	3.63	1159.3	N/A
1-B-300-40	3	300	26.2	136	28.2	3.6	56	10.2	13.5	4.5	72.1	9.9	1000	1500	3.00	3.03	94.6	4.5
1-B-300-70	2	300	25.8	133	27.9	3.6	55	10.2	13.5	4.5	72.7	9.3	1000	1500	3.00	3.04	116.3	3.9
1-B-300-120	2	300	26.5	136	28.6	3.5	57	10.1	13.5	4.5	72.2	9.8	1000	1500	3.00	3.05	122.3	5.1
1-B-300-200	3	300	26.2	136	28.4	3.6	58	10.3	13.5	4.5	72.1	9.9	1000	1500	3.00	3.06	142.1	6.9
1-B-300-350	2	300	26.5	136	28.5	3.5	56	10.2	13.5	4.5	72.2	9.8	1000	1500	3.00	3.10	195.6	6.9
1-B-300-600	3	300	25.7	134	27.7	3.7	55	10.2	13.5	4.5	72.5	9.5	1000	1500	3.00	3.10	213.7	7.5
1-B-500-40	2	500	31.5	143	33.5	3.1	54	10.4	13.5	4.5	72.2	9.8	1000	1500	3.00	3.11	252.5	1.4
1-B-500-70	3	500	30.8	142	32.7	3.0	57	10.2	13.5	4.5	72.1	9.9	1000	1500	3.00	3.15	333.6	1.6
1-B-500-120	2	500	30.1	142	32.2	3.1	53	10.3	13.5	4.5	71.9	10.1	1000	1500	3.00	3.21	423.9	1.7
1-B-500-200	3	500	30.1	142	32.2	3.1	52	10.3	13.5	4.5	71.9	10.1	1000	1500	3.00	3.23	479.9	1.5
1-B-500-350	2	500	30.7	142	32.7	3.0	53	10.1	13.5	4.5	72.1	9.9	1000	1500	3.00	3.28	548.4	2.1
1-B-500-600	3	500	31.5	143	33.5	2.9	53	10.1	13.5	4.5	72.2	9.8	1000	1500	3.00	3.29	563.3	2.7
2-B-.09-40	3	500	30.7	142	32.8	3.2	55	10.4	13.5	4.5	72.1	9.9	1000	1500	3.00	3.08	287.8	N/A
2-B-.09-70	2	500	30.9	142	33.0	3.0	55	10.2	13.5	4.5	72.2	9.8	1000	1500	3.00	3.22	370.6	N/A
2-B-.09-120	2	500	30.8	142	33.1	3.0	54	10.1	13.5	4.5	72.2	9.8	1000	1500	3.00	3.25	470.5	N/A
2-B-.09-200	3	500	30.9	142	33.2	3.1	57	10.3	13.5	4.5	72.2	9.8	1000	1500	3.00	3.29	543.2	N/A
2-B-.09-350	3	500	30.7	142	32.9	3.1	54	10.2	13.5	4.5	72.1	9.9	1000	1500	3.00	3.28	613.6	N/A
2-B-.09-600	2	500	31.0	142	33.1	2.9	57	10.0	13.5	4.5	72.2	9.8	1000	1500	3.00	3.38	671.6	N/A
Replicates of Run 1-A-500-120 for Reproducibility Calculations																		
1	3	500	30.0	141	32.0	3.2	56	10.3	13.5	4.5	72.2	9.8	1000	1500	3.00	3.44	811.1	N/A
2	2	500	30.5	142	32.4	3.2	57	10.3	13.5	4.5	72.0	10.0	1000	1500	3.00	3.46	748.1	N/A
3	3	500	30.0	142	32.0	3.2	58	10.3	13.5	4.5	71.8	10.2	1000	1500	3.00	3.45	807.2	N/A
4	2	500	30.5	142	32.5	3.2	58	10.3	13.5	4.5	72.0	10.0	1000	1500	3.00	3.43	788.3	N/A

APPENDIX C

Analysis of Nahcolite and Trona

STEP 1. - Sample Preparation.

A weighed sample of approximately 1.5 grams is placed in a 100 ml beaker, 70 ml of distilled water are added, and they are then stirred for 15 minutes. Water insoluble material is separated from the solution by passing the solution through a tared filtering crucible. The residue is washed with distilled water and the crucible and residue are weighed after being dried at 104° C for one hour. The filtrate is then diluted to volume in a 100 ml volumetric flask and retained for analysis.

$$\% \ H_2O \text{ insol.} = \frac{[(\text{wt. dried res.} + \text{crucible} + \text{paper}) - (\text{wt. dry crucible} + \text{paper})(100)}{\text{weight of sample}}$$

STEP 2. - Carbonate Determination.

A 20 ml. aliquot of filtrate from Step 1 is placed in a beaker and 20 ml. of distilled water are added. The solution is then titrated with 0.1 N HCl to a pH of 8.16 with the aid of a pH meter.

$$\% \ Na_2CO_3 = \frac{(\text{ml of HCl})(\text{normality of HCl})(10.6)}{(\text{sample wt, g})(\text{ml. of aliquot/ml of total vol.})}$$

STEP 3. - Bicarbonate Determination.

Using the solution from Step 2, the titration with 0.1 N HCl is continued to a pH of 4.0.

$$\% \ NaHCO_3 = \frac{[(\text{total ml HCl used}) - (2 \times \text{ml HCl from Step 2})] \ (\text{normality of HCl})(8.4)}{(\text{sample wt., g}) \ (\text{ml of aliquot/ml of total vol.})}$$

STEP 4. - Sulfur Determination.

The filtrate obtained from samples of reacted nahcolite and trona prepared in Step 1 was submitted for sulfur analysis by X-ray flourescence. Total sulfur present in the filtrate was reported as ppm SO_4. The weight percent SO_4 in the reacted sample was calculated as follows:

$$\% \ SO_4 = \frac{(\text{ppm } SO_4)(\text{mg})(0.1 \text{ liter})(100)}{(\text{ppm})(\text{liter})(\text{sample wt., mg})}$$

STEP 5. - Nitrate Determination.

Samples of reacted nahcolite and trona prepared in Step 1 were analyzed with an Orion specific nitrate ion electrode as described by A.S.T.M. procedure 419 B (19). The reported values of ppm NO_3 were converted as follows:

$$\text{wt } \% \ NO_3 = \frac{(\text{ppm } NO_3)(\text{mg})(0.1 \text{ liter})(100)}{(\text{ppm})(\text{liter})(\text{sample wt., mg})}$$

APPENDIX D

SO_2 Wet Test

The method used to check the accuracy of the Dupont 400 SO_2 analyzers was a modified form of the Shell-Thronton method (15). The modifications consisted of a vacuum tank system rather than a gas meter for gas volume determinations and the selection of methyl purple as an indicator in titrations. Calculations of the ppm SO_2 in the simulated flue gas are as follows:

The basic equation for parts per million by volume is

$$ppm = \frac{V_s}{V_t} (10^6),$$

where, V_s = volume of SO_2 measured, cu ft.

V_t = volume of flue gas sampled, cu ft.

The volume of SO_2 measured,

$$V_s = (4.178 \times 10^{-4})(N)(T),$$

where, N = normality of NaOH standard, gm-equiv/l

T = volume of NaOH used in titration, m.

The volume of gas sampled on a dry basis at standard conditions (for metered systems this would be the volume of dry gas measured, corrected to standard conditions),

$$V_t = 44.47 \frac{(P_2-P_1)(P_b-P_{mv})}{(P_b)(T_m)}$$

where, (P_2-P_1) = absolute tank pressure differential, test start to finish, inches of Hg.

P_b = barometric pressure, inches of Hg.

P_{mv} = saturated water vapor pressure at T_m, inches of Hg.

T_m = gas temperature in tanks, °R.

The resulting equation for ppm SO_2 in a sample is then

$$ppm = \frac{(9.393)(N)(T)(P_b)(T_m)}{(P_2-P_1)(P_b-P_{mv})}$$

REFERENCES

LIST OF REFERENCES

1. Ananth. K.P., Galeski, J.B., and Honea, F.I., Particle Emission Reactivity Report Prepared for U.S. EPA, Office of Research and Development, Washington, DC EPA-600/2-76-257 Sept. 1976.
2. Standards of Performance for New Stationary Sources, Federal Register, Vol. 36, Number 247, Part 60, December 25, 1971.
3. Perkins, Henry C., Air Pollution, McGraw-Hill, Inc., New York, NY, 1974.
4. Proposed Standards of Performance, Federal Register, Vol. 43, Number 182, Part 60, September 19, 1978.
5. Slack, A.V. and Holliden, G.A., Sulfur Dioxide Removal from Waste Gases, 2nd. Ed., Noyes Data Corp., Park Ridge, NJ, 1975.
6. Dulin, J.M., Rosar, E.C., Rosenberg, H.S., Anastas, M.Y., and Genco, J.M., The Use of Nahcolite Ore and Bag Filters for SO_2 Emission Control, Presented at the National Symposium, American Society of Mechanical Engineers, Air Pollution Control Division, Philadelphia, PA, August 25, 1973.
7. Doyle, Delmer J., "Fabric and Additive Remove SO_2", Electrical World, Vol. 187 #4 pages 32-34, Feb. 15, 1977.
8. Bechtel Corp. Evaluation of Dry Alkalis for Removing Sulfur Dioxide From Boiler Flue Gases. Final Report, EPRI FP-207, Research Project 491-1, San Francisco, CA, Oct., 1976.
9. Green, Richard, "Utilities Scrub Out SO_x", Chemical Engineering, Vol. 84, No. 11, page 102, May 23, 1977.

LIST OF REFERENCES--Continued

10. Personal communication with Orville B. Johnson, Project Manager, Coyote Station, Ottertail Power Company, Beulah, ND.

11. CE Plant Cost Index, Chemical Engineering, Vol. 85, No. 16, July 17, 1978.

12. Levenspiel, Octave, Chemical Reaction Engineering, John Wiley and Sons, Inc., New York, NY, 1967.

13. Szekely, J., Evans, J.W., and Sohn, H.Y., Gas - Solid Reactions, Academic Press, New York, NY, 1976.

14. Walas, S.M., Reaction Kinetics for Chemical Engineers, McGraw-Hill Book Company, New York, NY, 1959.

15. Gaksoyr, H. and Ross, K. The Determination of SO_3 in Flue Gases, Journal of the Institute of Fuel, Vol. 35, No. 255, pages 177-179, April 1962.

16. Howatson, J., Smith, J.W., Outka, D.A., and Dewald, H.D., Nahcolite Properties Affecting Stack Gas Pollutant Absorption, Proceedings of the 5th National Conference on Energy and the Environment, Cinncinatti, OH, Nov. 1-3, 1977.

17. Borgwardt, Robert H., "Kinetics of the Reaction of SO_2 with Calcined Limestone", Environmental Science and Technology, Vol. 4, No. 1, Jan. 1970.

18. Personal communication with George Montgomery, SEM Technician, Grand Forks Energy Technology Center, U.S. Department of Energy, Grand Forks, ND.

19. Standard Methods for the Examination of Water and Wastewater, 14th. Ed., American Public Health Assoc., American Water Works Assoc., and Water Pollution Control Federation, Washington, DC, 1976.

LIST OF REFERENCES--Continued

20. McCabe, W.L. and Smith, J.C., Unit Operations of Chemical Engineering, 3rd Ed., McGraw-Hill, Inc., New York, NY, 1976.

21. Fogler, H.S., The Elements of Chemical Kinetics and Reactor Calculations, Prentice-Hall, Inc., Englewood Cliffs, NJ, 1974.

22. Wine, R.L., Statistics for Scientists and Engineers, Prentice-Hall, Inc., Englewood Cliffs, NJ, 1964.